



## Research article

## Investigation of Wabe River water fitness for agricultural and industrial purposes

Tilahun Kasa<sup>a</sup>, Abeanezer Lukas Bassa<sup>a</sup>, Geleta Tilahun Negatu<sup>b</sup>, Zenebe Amele Sahile<sup>a</sup>, Daniel Reddythota<sup>a,\*</sup><sup>a</sup> Faculty of Water Supply & Environmental Engineering, AWTI, Arba Minch University, Ethiopia<sup>b</sup> Arba Minch Water Technology Institute, Arba Minch University, Ethiopia

## HIGHLIGHTS

- The Wabe River's irrigation index values show that the water is suitable for agriculture.
- In every sampling point over both seasons, the findings of the RSI, AI, and LSI are less than 9.
- Major contributors to sample site W4 contamination are urban wastewater and leachate.
- Gibb's figure shows that the origins of pollution are geological features and sediment influx.

## ARTICLE INFO

## Keywords:

Agriculture  
Hydrochemical composition  
Industrial purposes  
Wabe river  
Water quality indices

## ABSTRACT

The Wabe River is bordered by 74.84% agricultural area, and farmers rely solely on rainfall. The present research made an attempt to investigate the suitability of the Wabe river water for Agricultural and Industrial purpose. The suitability of river water for agricultural use was evaluated using the sodium adsorption ratio (SAR), potential salinity (PS), magnesium ratio (MR), Kelly index (KI), permeability index (PI), residual sodium carbonate (RSC), sodium percentage (%Na), and heavy metal pollution index (HPI). Additionally, the Ryznar Stability Index (RSI), Aggressive Index (AI), and Langelier Saturation Index (LSI) were used to evaluate the river water's suitability for industrial uses. Furthermore, plot the Gibb's diagrams to identify the sources of pollution and Piper diagrams to determine the hydrochemical composition of Wabe water. According to the HPI, pollution levels in the wet and dry seasons ranged from 53.34 (low) to 317.58 (medium) and 32.24 to 102.42 (low), respectively. The results showed that the Wabe River has very acceptable water quality characteristics and that the trace elements identified did not surpass thresholds that made them dangerous for agricultural usage. The findings showed that domestic wastewater and leachate contamination at sampling point W4 is the cause of the water quality deterioration in the downstream zone. The Ryznar Stability Index (RSI), Aggressive index, and Langelier saturation index readings were less than 9 at all sampling locations during both seasons, suggesting that the river water was corrosive, highly aggressive and unusable for industrial use without treatment.

## 1. Introduction

Rivers and lakes are the principal surface water resources most accessible to human consumption, irrigation and industrial uses (Ustaoglu et al., 2021; Shil et al., 2019). Due to the rapid increase in human population, urbanization, and industrialization, these freshwater resources are being abused (Menberu et al., 2021). However, because of water pollution and climate change during the past 10 years, the water deficit has expanded to be a worldwide problem (Ustaoglu et al., 2020).

Water pollution poses a threat to the long-term sustainability of water resources, human existence, and socioeconomic growth (Ustaoglu and Tepe, 2019). It also results in water scarcity, decreased agricultural crop production, tainted food chains, illnesses, and the demise of aquatic life (Egbueri et al., 2021).

Wabe River is one of the prime sources of drinking and irrigation for the nearby communities throughout the stretch. Wabe River is one of the rivers in the Gurage zone of southern Ethiopia flows across the urban areas and ends up into the Omo-Gibe basin. A number of anthropogenic

\* Corresponding author.

E-mail addresses: [daniel.reddy@amu.edu.et](mailto:daniel.reddy@amu.edu.et), [dr.dany77@gmail.com](mailto:dr.dany77@gmail.com) (D. Reddythota).<https://doi.org/10.1016/j.heliyon.2022.e11865>

Received 2 August 2022; Received in revised form 1 November 2022; Accepted 17 November 2022

2405-8440/© 2022 The Author(s). Published by Elsevier Ltd. This is an open access article under the CC BY-NC-ND license (<http://creativecommons.org/licenses/by-nc-nd/4.0/>).

and natural activities, including agricultural runoff water (Ustaoglu et al., 2021; Terfasa et al., 2019; Parris, 2011), domestic wastewater (Preisner, 2020; Ustaoglu and Tepe, 2019), dumping of solid waste in canals and inappropriate locations (Menberu et al., 2021; Egbueri et al., 2021; Weldeyohannis et al., 2020), urban sediment inflow (Egbueri, 2022; Sahle et al., 2019; Ustaoglu and Tepe, 2019), river flows through lithogenic structures (Asnake et al., 2021), and soil erosion (Reddythota and Timotewos, 2022; Terfasa et al., 2019), have a negative impact on the water quality over time. These surface water resources are no longer suitable for drinking, industrial, agricultural, and other applications due to water quality degradation (Egbueri et al., 2021; Ustaoglu et al., 2020; Hamid et al., 2020; Şener et al., 2017).

On plant growth and crop productivity, the crucial levels of salts in the water have a detrimental effect (Zaman et al., 2018; Etteieb et al., 2017; Manuel et al., 2017). Water quality plays a vital role in food, beverage and pharmaceutical industries where the end product is intended to be consumed by the consumer. Pollutants will seep through the product, seriously endangering the user. Food spoilage has an impact on food color, texture, and edibility as well as nutritional value due to physical, chemical, and biological pollutants (Amit et al., 2017). In addition, contaminated water damages processes and corrodes pipes, boilers, and process units (Egbueri et al., 2022). Enhancement of agricultural activities and establishment of industries are essential to have suitable water (Egbueri, 2022; Ustaoglu et al., 2021). As a result, assessments of water quality and characterizations of hydrochemical composition are now crucial components of studies, planning, and management of water resources (Manea et al., 2019). A water quality index is a mathematical technique for reducing a large amount of data on water quality to a single number that expresses the condition of the water quality of the water resource (Menberu et al., 2021). The major percentage of farmers is still depending on the rain water rather than the Wabe river water for agricultural activities. In rain-fed agricultural systems, the yield of crops is significantly impacted by the seasonal variations of rainfall (Edo Harka et al., 2021). The Wabe River will solve the water challenges for agricultural activities, if the water quality is suitable. The goal of this study is to use a variety of water quality indices to determine whether the Wabe River water is suitable for industrial and agricultural use.

The aim of the present study is to (i) evaluate the spatial and seasonal changes of physicochemical and heavy metals parameters affecting the water quality of Wabe River, (ii) applying multiple irrigation water quality indices, industrial purposes suitability indices, and heavy metal pollution indices to evaluate the suitability of river water for irrigation and industrial applications during the wet and dry seasons, (iii) calculate the irrigation water quality of the river with sodium adsorption ratio (SAR), potential salinity (PS), magnesium ratio (MR), Kelly index (KI), permeability index (PI), residual sodium carbonate (RSC), and sodium percentage (Na%) indexes, and (iv) determine the heavy metal values in the water with heavy metal pollution index (HPI) index to evaluate in terms of public health. (v) calculate the water quality of the river for industrial purposes with Langelier Saturation Index (LSI), Aggressive Index (AI), and Ryznar Stability Index (RSI) indexes (vi) piper diagrams were used to determine the hydrochemical makeup of the contaminants in the water, and Gibb's diagrams were used to evaluate the causes of pollution. The Wabe River's water quality state and sources of contamination have never before been thoroughly examined in one study, which will serve as a benchmark for potential future studies.

## 2. Methodology

### 2.1. Description of Study Area

Wabe River flows from the west to the southwest of south-central Ethiopia, near wolkite town and 178 km from the capital city of Addis Ababa. The Wabe River originates in the Gurage mountain range and flows into the Gibe River, which is one of the Omo-Gibe basin's sub-catchments (Legese et al., 2019). The Wabe River catchment is located

at 08°21'30"–08°30'00"N, and 37°49'00"–38°05'40"E (Figure 1). The catchment covers an area of 1860 km<sup>2</sup> and has elevations ranging from 1014 to 3611 m. The river is 91 km long, with an average annual flow of 30.4 m<sup>3</sup>/s. Wabe River watershed is categorized as belonging to the woinadega zone in accordance with Ethiopia's agroecological categorization. The dry and rainy seasons last from November to May and June to October, respectively, and the Wabe catchment region receives 70–90% of its annual rainfall from June to September. The highest temperature is between 20 °C (during the rainy season) and 39 °C (in the dry season). While the minimum temperature ranges from 0 °C to 19 °C. The average temperature is 18 °C and the mean annual rainfall ranges between 1111 to 1374mm (Sahle et al., 2019).

The upper and middle portions of the watershed have porous, well-draining soils, but the lower part has poor drainage and less permeable soils. In the Wabe River watershed, there are four main types of soil: loam, loam (huntsol), clay, and sandy loam. In the river watershed, Clay and Sandy Loam are the two most prevalent soil types (Namara et al., 2022). On the other hand, the geologic condition of the catchment near to 90% is covered by tertiary volcanic rock as a part of Omo-Gibe River basin.

The Wabe River watershed has a variety of different land uses and land cover types, including areas with rocks, aquatic vegetation, irrigated cropland, rain-fed agricultural land, floodplains, and areas with forests, water bodies, shrub land, wood land, grass land, settlement areas, bare land, and isolated trees. The majority of the watershed areas were covered with agricultural or rain-fed cropland types of land. 74.84% of the area is covered by agricultural land that receives water from rain.

There are two districts in the south-west shoa zone and six districts in the gurage zone in the Wabe River basin (Oromia region). The municipalities in the Gurage zone's catchment area include Abeshge, Cheha, Kabena, Kokir, Ezha, and Mehur Aklil. The Gurage zone's catchment area has a total population of 537423 people (CSA Central Statistics Agency, 2017). The two Oromia region districts where a portion of the watershed is located are Woliso and Saden Soddo. Districts in the south-west shoa zone have 318074 people living in them (CSA Central Statistics Agency, 2017). Most of peoples life within the catchment depends on agriculture.

### 2.2. Sample site selection and sampling

Sampling sites were selected in the Wabe River based on the ease and reliability of the access, irrigation practices, human settlements and waste disposal activities (Figure 1). During the wet (July, August and September) and dry (November, December and January) seasons, water samples were collected by time-pace composite sampling method at a depth of 30 cm from the surface on 10 selected sampling locations (T1, T2, T3, T4, W1, W2, W3, W4, W5, and W6). Five samples were collected and make it as a composite sample at each sampling point during both seasons in 2021. Garmin model 60 was used to determine the geographic locations of sampling points. The 1.5 L polyethene bottles were thoroughly cleansed and rinsed with 2 ml HCl. The bottles were cleaned with sample water before being labelled properly. The water sample was preserved in a 4 °C icebox for 24 h before being transported to Arba Minch University's water quality laboratory for analysis, following to APHA (2012) sampling technique.

### 2.3. Analysis of physicochemical water quality parameters

EC, pH, TDS, and temperature were measured at *in-situ* by portable multimeter (HQ40D, USA) for each sample and the remaining nine parameters were analyzed in the Arba Minch Water Quality Laboratory. The titrimetric method was used to determine total hardness, carbonates (CO<sub>3</sub><sup>2-</sup>) and bicarbonates (HCO<sub>3</sub><sup>-</sup>). The Argentometric method was used to assess Chlorides. Sulfates (SO<sub>4</sub><sup>2-</sup>) by Spectrophotometric method (UV-VIS spectrometer, India), Sodium (Na<sup>+</sup>) and Potassium (k<sup>+</sup>) by Flame Photometric method (02655-10, Flame photometer, India) and Calcium (Ca<sup>2+</sup>) & Magnesium (Mg<sup>2+</sup>), Copper (Cu<sup>2+</sup>), Cadmium (Cd<sup>2+</sup>), and Zinc (Zn<sup>2+</sup>) ions were determined by FAAS (BUCK Scientific 210 VGP, USA).

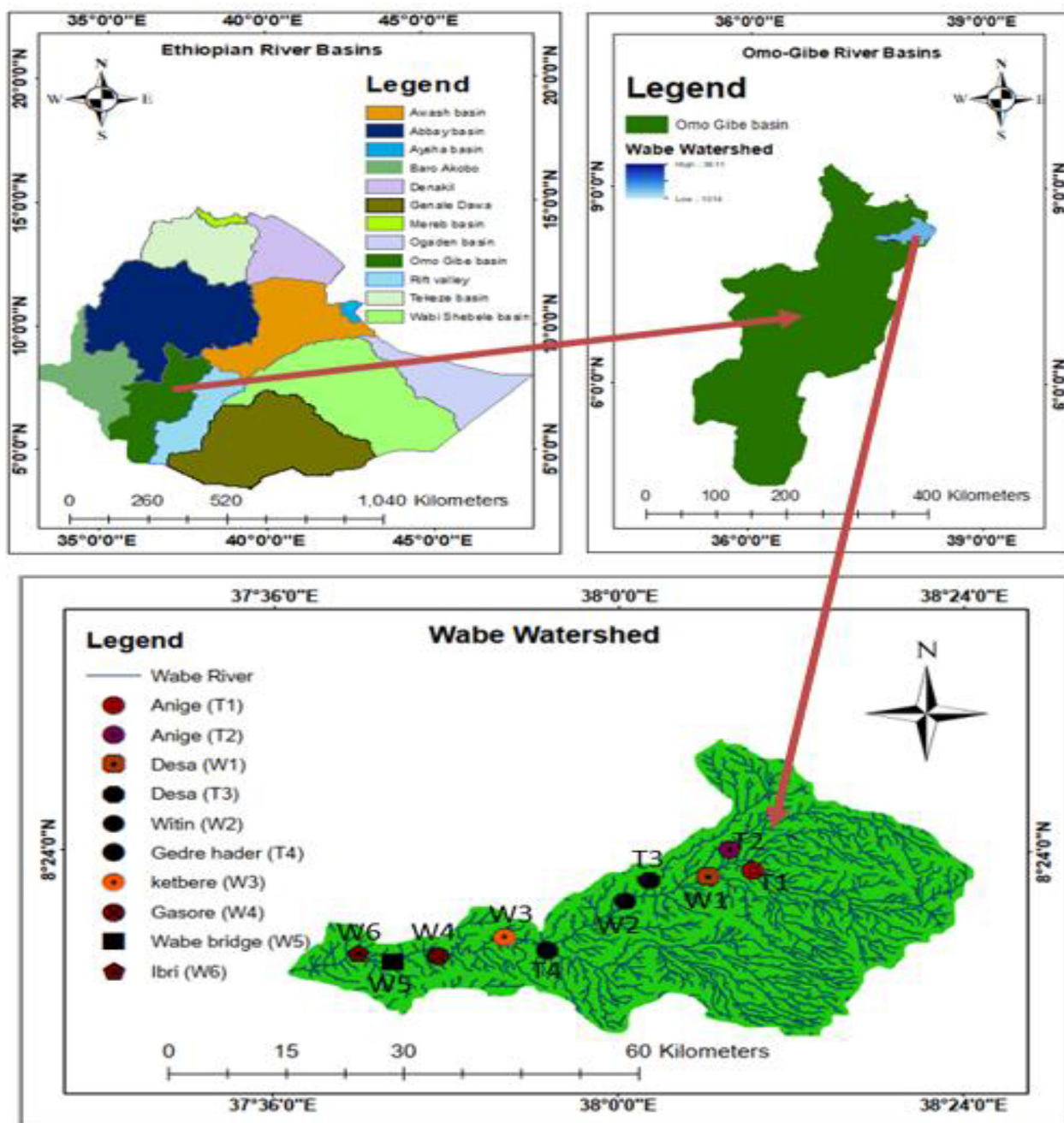


Figure 1. Location map of the study area.

2.4. Kaiser–Meyer–Olkin and Bartlett tests

The Kaiser–Meyer–Olkin (KMO) and Bartlett tests were employed to see if the data was suitable for Principal Component Analysis (PCA). Kaiser–Meyer–Olkin (KMO) and Bartlett’s tests were used to determine the data suitability to execute the PCA (Child, 2006). KMO is a measure of sample adequacy using Eq. (1). If only KMO value is greater than 0.5, PCA can be used. Bartlett’s test measures the relationship between the variables at a significance level.

$$KMO = \frac{\sum_i \neq j^2 r_{ij}}{\sum_i \neq j^2 r_{ij} + \sum_i \neq j^m} \tag{1}$$

where as  $r_{ij}$  is the correlation matrix;  $U = [u_{ij}]$  is the partial covariance matrix;  $\Sigma$  = summation notation.

2.5. Principal component analysis (PCA)

Principal Component Analysis (PCA) is a method for reducing the dimensionality of datasets and obtaining major information based on the original variables with no overlap. PCA was used to identify the key components and sources in various seasons, which accurately indicate the level of pollution in a water body. It is important to note that the results of these analyses are divided into three categories, much like a straightforward correlation analysis. Component loadings below 0.50 are regarded as weak and inconsequential, but loadings between 0.50 and 0.75 are regarded as moderate and significant. Strong (high) loadings are encountered in ranges greater than 0.75. Strong loadings are typically considered to be extremely significant and to explain more specifics about a particular dataset (Egbueri et al., 2022). The PCA analysis was performed using SPSS 20.0 software.

2.6. Hydro-chemical characteristics of Wabe river water

The ionic compositions of river water samples were explored and the type of surface water was generated by using AqQA1.5 software. The analytical values were plotted on a piper diagram during both dry and wet seasons to determine the hydrochemical compositions of the river water and water type. Gibbs diagrams were used intuitively to judge the effect of these influences on the key chemical composition of river water. MS EXCEL version 2016 was utilized to create the Gibbs diagram in this investigation.

2.7. Suitability for irrigation use

Water's fitness for agricultural use is determined by a variety of physicochemical parameters, principally dissolved salts (Shil et al., 2019). The state and suitability of the Wabe river water for irrigation were determined using various water quality indices such as SAR, PI, MR, KI, RSC, PS, and %Na. Wilcox diagrams were also used to examine the appropriateness of water for irrigation purposes using Wilcox diagram software 6.7. Table 1 shows the summary of equations used for various irrigation water quality indices and water quality classification.

2.8. Heavy metal pollution index (HPI)

Surface water pollution can be measured using the heavy metal pollution index (HPI), which measures the combined and individual effects of heavy metals on water quality. This HPI is used to determine the level of contamination in river water due to irrigation usage. The following Eq. (2) can be used to calculate HPI.

$$HPI = \frac{\sum_{i=1}^n WiQi}{\sum_{i=1}^n Wi} \tag{2}$$

where, Wi is the given weightage of each heavy metal, with a value ranging from 0 to 1. 'n' is the total number of heavy metals; Qi is the quality rating of each heavy metal estimated by Eq. (3).

Table 1. Equations for Irrigation water quality indices and index value with category classification.

Index	Equation	Value	Category
SAR	$SAR = \frac{Na^+}{\sqrt{\frac{Ca^{2+} + Mg^{2+}}{2}}}$	<20	Excellent
		20–40	Good
		40–60	Permissible
		60–80	Doubtful
		>80	Unsuitable
Potential Salinity (PS)	$PS = Cl^- + \frac{1}{2} SO_4^{2-}$	< 3	Suitable
		>3	Unsuitable
Magnesium Ration (MR)	$MR = \frac{Mg^{2+} * 100}{Ca^{2+} + Mg^{2+}}$	<50	Suitable
		>50	Unsuitable
Kelly Index (KI)	$KI = \frac{Na^+}{Ca^{2+} + Mg^{2+}}$	<1	Suitable
		>1	Unsuitable
Residual Sodium Carbonate (RSC)	$RSC = (CO_3^{2-} + HCO_3^-) - (Ca^{2+} + Mg^{2+})$	<1.25	Suitable
		1.25–2.5	Marginally Unsuitable
		>2.5	Unsuitable
Permeability Index (PI)	$PI = \frac{Na^+ + HCO_3^-}{Ca^{2+} + Mg^{2+} + Na^+} * 100$	<25	Unsuitable
		25–75	Good
		>75	Excellent
Sodium Percentage (%Na)	$\% Na = \frac{Na^+ * 100}{Ca^{2+} + Mg^{2+} + Na^+ + K^+}$	<60	Safe
		>60	Unsafe

Source: Berhe (2020); Shil et al. (2019)..

$$Qi = \frac{Vi}{Si} * 100 \tag{3}$$

where Vi denotes the measured concentration of each heavy metal and Si denotes the heavy metals' standard limits (Hasan et al., 2020). FAO irrigation water quality standards were used in this study.

2.9. Suitability for industrial use

Water is required by companies for a variety of reasons, including processing, cooling, boiler feeding, and sanitary purposes. Certain industries require high-quality water that is free of scale and corrosion. In heavy industries, scale formation is a serious challenge (Wali et al., 2020). In 1936, Langelier created the Langelier Saturation Index (LSI) to analyze the scale growing capacity of various water qualities. The LSI was estimated by Eq. (4) as (pHs) is the difference between the real pH of the water and the saturated pH with calcium carbonate (Shil et al., 2019) by Eq. (5).

$$LSI = pH(\text{saturated}) - pHs \tag{4}$$

$$pHs = A + B - C - D \tag{5}$$

The pHs A, B, C, and D are calculated using Langelier's method. If the LSI value is negative, the water has a limited propensity for scaling. If the LSI is positive, the water is more likely to develop scales. Langelier also developed the aggressive index (AI), which is used to measure water corrosivity. Because it ignores the effects of temperature, the AI is simpler and more convenient than the LSI (Shil et al., 2019). Table 2 shows the LSI and AI category-based results. AI was estimated by Eq. (6).

$$AI = pH(\text{actual}) + C + D \tag{6}$$

where, the values C and D are determined using Langelier's method.

To minimize misinterpretation of the positive saturation index, Ryznar created the stability index (SI). The Ryznar stability index (RSI) is calculated by Eq. (7) as follows:

$$RSI = 2pHs - pH \tag{7}$$

Where pH is the solution's measured pH, and pHs is the pH at saturation point calculated using Langelier's method. The stability index value is always positive for all waterways (Wali et al., 2020). Table 3 shows the water classifications based on the Ryznar stability index.

3. Results and discussions

3.1. Water quality

Water quality is extremely important to all living organisms on the planet. Pollution sources, climatic circumstances, geographical conditions, location and time will have an impact on water quality (FAO, 2015). The water quality of the Wabe river is determined by temperature, pH, electrical conductivity (EC), total dissolved solids (TDS), Calcium, Magnesium, Sodium, Potassium, Chlorides, Sulfates, carbonates, bicarbonates, total hardness (TH), Cadmium, Copper and Zinc (Table 4).

Table 2. Classification of water suitability based on LSI and AI.

Corrosive characteristics and categories	Langelier index ranges (LSI)	Aggressive index (AI) ranges
Highly aggressive	< -2	< 10
Moderately aggressive	-2 to 0	10 to 12
Non-aggressive	> 0	> 12

**Table 3.** Category of water-based on RSI.

RSI	Inferences	RSI	Inferences
<5.5	Heavy scale will form	4–5	Heavy scale
5.5–6.2	Scale will form	5–6	Light scale
6.2–6.8	No difficulties	6–7	Little scale or corrosion
6.8–8.5	Water is aggressive	7–7.5	Corrosion significant
>8.5	Water is very aggressive	7.5–9	Heavy corrosion
		>9	Corrosion intolerable

**3.1.1. Temperature and pH**

The temperatures of the Wabe river water samples were in the range of 18 °C (T1) to 23.45 °C (W4) and 21 °C (T2) to 26.5 °C (W4) during the wet and dry seasons, respectively (Table 4). Temperatures varied

significantly by season, dry season samples have considerably higher than the rainy season. Wabe River Stream water reached its lowest temperature at recorded from the upstream and the maximum temperature from the downstream. The contamination of domestic wastewater and leachate may be the cause of the greater temperature in the downstream. The rate of mineral dissolution has been found to tend to rise with rising water temperature, despite the fact that there is no set standard limit for temperature (WHO World Health Organization, 2008; Egbueri et al., 2019). Temperature influences the rate of chemical and biological reactions in river water (Ficklin et al., 2013). Warming temperatures due to climate change will affect plant growth and development with crop yield (Hatfield and Prueger, 2015).

The pH values of the water samples were in the range of 6.63 (W4) to 7.5 (W5) and 7.42 (W2) to 8.5 (W4) during the wet and dry seasons, respectively (Table 4). The sample points W4 and W2 recorded the lowest

**Table 4.** Summary of results obtained from both laboratory and field measurement.

Parameter	Period	T1	T2	T3	T4	W1	W2	W3	W4	W5	W6
Temperature	Wet	18 ± 0.2	20.2 ± 1.4	20.6 ± 2.3	19 ± 1.2	21 ± 2.2	20.3 ± 0.3	21.9 ± 0.3	23.45 ± 1.2	21 ± 2.4	22 ± 0.57
	Dry	23 ± 1.2	21 ± 2.4	25 ± 0.5	22 ± 1.4	24 ± 0.8	23 ± 1.4	25 ± 4	26.5 ± 2.5	24 ± 1.8	23.5 ± 3
TDS	Wet	64.7 ± 8.7	<b>55 ± 12.1</b>	76 ± 7	47.46 ± 15.7	58.1 ± 12.8	66.7 ± 16.2	74 ± 6.55	<b>85.3 ± 9.6</b>	65.8 ± 8.9	53 ± 8.2
	Dry	135 ± 19.5	<b>115 ± 9.3</b>	163 ± 18.9	137.7 ± 15.2	147 ± 13	165.3 ± 18.5	177 ± 21.6	162 ± 26.3	<b>204.7 ± 17.4</b>	171.67 ± 24.8
E.C	Wet	119 ± 16.4	105.7 ± 10.4	135.3 ± 12.05	<b>101.3 ± 17.6</b>	112.6 ± 23.7	125 ± 19.5	136 ± 15.1	<b>151 ± 13</b>	120.6 ± 15.3	104 ± 9.2
	Dry	215 ± 32.8	<b>190.3 ± 17.6</b>	264.7 ± 29.8	219.3 ± 28.7	240 ± 22.2	265 ± 35	287 ± 30	255 ± 38	<b>325 ± 20</b>	275 ± 31.2
pH	Wet	7.3 ± 0.17	7.16 ± 0.15	7.1 ± 0.076	7.4 ± 0.11	7.03 ± 0.15	7.37 ± 0.3	7.2 ± 0.46	<b>6.63 ± 0.2</b>	<b>7.5 ± 0.25</b>	7.1 ± 0.2
	Dry	8.07 ± 0.5	7.6 ± 0.26	8.23 ± 0.57	7.75 ± 0.56	7.96 ± 0.72	<b>7.42 ± 0.09</b>	8.2 ± 0.26	<b>8.5 ± 0.5</b>	7.8 ± 0.72	8.1 ± 0.3
TH	Wet	<b>58 ± 7.2</b>	67.3 ± 8.3	82.7 ± 10	72 ± 7.2	63.3 ± 5.7	72 ± 2	94.7 ± 9.2	<b>106.7 ± 7.5</b>	84 ± 8	63.3 ± 5.77
	Dry	<b>26.7 ± 4.2</b>	30 ± 5.3	44.7 ± 6.4	34 ± 9.2	45.3 ± 4.6	40 ± 7.2	50.7 ± 11.5	42 ± 7.2	<b>55.3 ± 8.1</b>	48 ± 4
Chloride	Wet	20.35 ± 3.57	24.14 ± 1.42	33.1 ± 3.27	<b>17.5 ± 5.73</b>	26.98 ± 4.26	32.2 ± 4.1	35.97 ± 2.95	<b>42.6 ± 2.84</b>	36.45 ± 7.82	26.5 ± 2.16
	Dry	<b>27 ± 3.75</b>	34 ± 3.7	42.6 ± 5.12	52.54 ± 1.42	35.97 ± 5.9	45.44 ± 2.46	50.2 ± 8.07	54.4 ± 2.2	48.75 ± 2.95	<b>64.37 ± 4.4</b>
Ca	Wet	<b>10.7 ± 1.49</b>	14.02 ± 2.77	18.5 ± 3.05	15.2 ± 3.17	14 ± 2.06	19.3 ± 5.04	22.3 ± 2.78	<b>24 ± 13.3</b>	17.2 ± 1.23	15.8 ± 1.6
	Dry	<b>5.2 ± 1.8</b>	9.4 ± 3.4	8.3 ± 1.3	10.85 ± 1.5	8.6 ± 1.75	10.4 ± 1.85	<b>13.45 ± 2.3</b>	11.6 ± 1.9	12.4 ± 2.97	13.36 ± 1.75
Mg	Wet	7.2 ± 1.4	6.15 ± 0.8	8.6 ± 0.5	<b>4.42 ± 1.35</b>	6.18 ± 1.19	7.06 ± 1.5	9.5 ± 1.2	8.7 ± 2.4	<b>10.1 ± 2.4</b>	6.7 ± 1.06
	Dry	3 ± 0.3	2.06 ± 0.3	4.76 ± 0.37	<b>1.52 ± 0.42</b>	4.9 ± 0.69	3.71 ± 0.9	3.4 ± 0.7	3.8 ± 0.24	<b>6.07 ± 0.6</b>	3.7 ± 0.99
Sulphate	Wet	<b>11.7 ± 3.5</b>	14.37 ± 6.65	26.57 ± 9.3	15.3 ± 12.7	19.4 ± 6.3	29.7 ± 8.8	25.7 ± 7.8	<b>35.1 ± 18.7</b>	26.8 ± 9.6	18.4 ± 5.03
	Dry	3.72 ± 0.22	<b>3.4 ± 0.14</b>	7.61 ± 1.58	5.27 ± 0.72	4.5 ± 0.46	9.62 ± 0.23	3.64 ± 0.32	7.5 ± 0.24	<b>10.2 ± 0.69</b>	3.53 ± 1.9
Bicarbonate	Wet	<b>32.7 ± 5</b>	40.6 ± 7.57	57.33 ± 12.2	34 ± 7.2	45.3 ± 3.05	39.3 ± 2.3	58.67 ± 11.54	53.3 ± 10.06	<b>62.7 ± 8.3</b>	48 ± 16
	Dry	14.7 ± 3.1	18 ± 4	13.3 ± 5	10 ± 2	16.7 ± 6.1	11.3 ± 3.05	17.3 ± 3	12 ± 2	<b>26.7 ± 8.1</b>	<b>9.3 ± 2.3</b>
K	Wet	2.2 ± 0.5	2.5 ± 0.1	3.7 ± 0.42	<b>1.8 ± 0.6</b>	2.8 ± 0.36	2.5 ± 0.5	3.4 ± 0.32	<b>4.2 ± 0.6</b>	2.7 ± 0.2	1.76 ± 0.47
	Dry	1.4 ± 0.05	1.7 ± 0.2	1.6 ± 0.1	<b>0.9 ± 0.1</b>	1.23 ± 0.06	1.76 ± 0.2	2 ± 0.3	<b>2.8 ± 0.9</b>	2.2 ± 0.5	1.4 ± 0.35
Na	Wet	8.4 ± 1.4	7.2 ± 2.2	11.5 ± 2.3	7.5 ± 1.05	9.5 ± 1.8	10.9 ± 1.9	13.2 ± 2.2	10.8 ± 1.66	14.5 ± 2.2	8.5 ± 1.2
	Dry	11.5 ± 2.3	14.7 ± 2.08	18 ± 3.6	12.7 ± 1.53	18.7 ± 4.04	18.7 ± 6.8	21.3 ± 4.5	15.7 ± 1.52	24.8 ± 3	19.7 ± 1.15
Cd <sup>2+</sup> (mg/L)	Wet	0.007 ± 0.07*	<b>0.005 ± 0.06*</b>	0.009 ± 0.05*	0.006 ± 0.07*	0.008 ± 0.04*	0.012 ± 0.08*	0.010 ± 0.03*	<b>0.032 ± 0.09*</b>	0.018 ± 0.04*	0.012 ± 0.03*
	Dry	0.005 ± 0.04*	<b>0.003 ± 0.07*</b>	0.006 ± 0.07*	<b>0.003 ± 0.02*</b>	0.006 ± 0.04*	0.007 ± 0.04*	0.0045 ± 0.03*	0.0084 ± 0.04*	<b>0.01 ± 0.04*</b>	0.006 ± 0.04*
Cu <sup>2+</sup> (mg/L)	Wet	<b>0.18 ± 0.19*</b>	0.25 ± 0.02	0.33 ± 0.05	0.24 ± 0.0375	0.19 ± 0.04	0.32 ± 0.054	0.45 ± 0.06	<b>0.6 ± 0.06</b>	0.52 ± 0.12	0.43 ± 0.05
	Dry	<b>0.11 ± 0.04</b>	0.16 ± 0.08	0.22 ± 0.06	0.18 ± 0.12	0.132 ± 0.13	0.224 ± 0.03	0.27 ± 0.07	0.3 ± 0.06	<b>0.32 ± 0.03</b>	0.19 ± 0.04
Zn <sup>2+</sup> (mg/L)	Wet	0.095 ± 0.01	0.115 ± 0.02	0.185 ± 0.03	<b>0.08 ± 0.02</b>	0.115 ± 0.05	0.171 ± 0.01	0.108 ± 0.04	0.207 ± 0.04	<b>0.271 ± 0.02</b>	0.13 ± 0.04
	Dry	<b>0.048 ± 0.01</b>	0.073 ± 0.03	0.115 ± 0.02	0.05 ± 0.02	0.089 ± 0.03	0.131 ± 0.03	0.067 ± 0.02	0.182 ± 0.02	<b>0.214 ± 0.03</b>	0.08 ± 0.04

average values of 6.63 and 7.42 throughout the rainy and dry seasons, respectively. The lowest results were most likely attributable to the entry of commercial garbage from the town (Angello et al., 2021) as well as the inflow of leachate from the disposal site during the rainy season. The lowest value of W4 during the rainy season was caused by the decomposition of organic materials in the town's wastewater. It's possible that local car garages and car wash facilities will also contribute waste. The highest values were seen during the dry season, possibly due to aerobic respiration of aquatic organisms (Hamid et al., 2020). Acidic pH depletes calcium, magnesium and potassium, all of which are necessary for plant growth (Egbueri et al., 2021; Neina, 2019). The current readings, in contrast to irrigation water quality specifications, were within the acceptable range (6.5–9) (Goher et al., 2014).

3.1.2. Electrical conductivity (EC) and total dissolved solids (TDS)

Two important markers for determining the degree of deterioration in water quality are the TDS and EC of the water (Egbueri et al., 2022). During the wet and dry seasons, electrical conductivity values ranged from 101.3 µs/cm to 151 µs/cm and 190.3 µs/cm to 325 µs/cm, respectively. During the wet and dry seasons, TDS levels were 55 mg/L (T2) to 85.3 mg/L (W4) and 115 mg/L (T2) 204.7 mg/L (W5), respectively (Table 4). During the wet season, W4 had the highest average TDS and EC due to runoff inflow from both urban and rural regions (Angello et al., 2021; Bouslah et al., 2017); as well as leachate from a nearby landfill site (Angello et al., 2021; Bouslah et al., 2017; Mekonnen et al., 2020). High temperatures accelerated evaporation and increased ionic content in river water throughout the dry period, resulting in the highest mean value (Ngabirano et al., 2016). Both EC and TDS were within the FAO guidance line (3000 µs/cm and 2000 mg/L) for irrigation purposes during both research periods (Goher et al., 2014). There is an increased tendency for home appliances such as heaters, boilers, and water distribution systems to scale, with TDS >1000 mg/L (Egbueri et al., 2019).

3.1.3. Calcium and magnesium

During the wet and dry seasons, calcium concentrations ranged from 10.7 mg/L (T1) to 24 mg/L (W4) and 5.2 mg/L (T1) to 13.45 mg/L (W4), respectively. During the wet and dry seasons, magnesium levels were 4.42 mg/L (T4) to 10.1 mg/L (W5) and 1.52 mg/L (T4) to 6.7 mg/L (W5), respectively (Table 4). Increased values were most likely related to the inflow of household waste and the weathering of rock during the rainy season (Aliyu et al., 2020). The highest average value was presumably connected to the ion exchange process during the dry season (Rawat

et al., 2018). However, both calcium and magnesium (400 and 60 mg/L, respectively) were within the irrigation guidelines (Goher et al., 2014).

3.1.4. Sodium and potassium

Sodium concentrations in the wet and dry seasons varied from 7.2 (T2) to 14.5 (W5) mg/L and 11.5 (T1) to 24.8 (W5) mg/L, respectively. Potassium values in the rainy and dry seasons ranged from 1.8 mg/L (T4) to 4.2 mg/L (W4) and from 0.9 mg/L (T4) to 2.8 mg/L (W4), respectively (Table 4). Weathering of rock, soil erosion, and runoff from agricultural land may all contribute to the maximum value during the rainy season (Saha et al., 2019). The greatest value observed during the dry sample event could be due to reduced river water flow and the ion exchange mechanism (Hamid et al., 2020). Sodium levels were within the range for both seasons when compared to irrigation water quality guidelines. During the wet season, however, potassium was only safe for irrigation at T4 and W6. Except for study sites W4 and W5, all sample sites were safe for irrigation during the dry season. The low EC values are consistent with the low Cl<sup>-</sup> and Na<sup>+</sup> ion concentrations found in all of the water samples. When SO<sub>4</sub><sup>2-</sup> is present in water in excess levels, it can clog pipes and cause health problems including diarrhea (Sylus and Ramesh, 2018).

3.1.5. Chloride and sulfate

Chloride concentrations ranged from 17.5 (T4) to 42.6 (W4) mg/L and 27 (T1) to 64.37 (W6) mg/L during the wet and dry seasons, respectively. Sulfate concentrations ranged from 11.7 (T1) to 35.1 (W4) and 3.4 (T2) to 10.2 (W5) mg/L during the wet and dry seasons, respectively (Table 4). Runoff from nearby agricultural land and domestic trash from the town might be the reason for the higher values during the wet season (Şener et al., 2017). The greatest readings in the dry season sampling points could be due to excessive evaporation, a drop in river water volume, or the discharge of ions from the bottom deposits (Aliyu et al., 2020). However, anthropogenic activities such improper waste disposal in dumpsites, sewage, and agriculture flows could have an impact on the amount of chloride in water (Egbueri, 2018; Mukate et al., 2017). The quantities of SO<sub>4</sub><sup>2-</sup> in water may be affected by human-induced activities such as the application of fertilizer to crops and the use of detergent in homes (Kadam et al., 2021). According to the FAO, the maximum allowable limit of chloride and sulfate for irrigation usage is 1063 and 960 mg/L, respectively (Goher et al., 2014). Both chloride and sulfate were found to be safe during both sample periods when compared to the irrigation recommendation. Geogenic processes include rock weathering, mineral dissolution, and the breakdown of sulfide and carbon-based materials can also have an impact on SO<sub>4</sub><sup>2-</sup> and Cl<sup>-</sup> (Egbueri et al., 2019; Kadam et al., 2021).

3.1.6. Bicarbonates

HCO<sub>3</sub><sup>-</sup>, CO<sub>3</sub><sup>2-</sup>, and OH<sup>-</sup> ions, which can neutralize water, are the main sources of Total Alkalinity in natural water (Aydin et al., 2020). Bicarbonate concentrations in Wabe river water samples ranged from 32.7 mg/L (T1) to 62.7 mg/L (W5) and 9.3 mg/L (W6) to 26.7 mg/L (W5) during the wet and dry seasons, respectively (Table 4). Carbonates were not present in all sampling points. Carbonate and bicarbonate ions are in a dynamic equilibrium with carbonic acid in a certain quantitative proportion, establishing a chemical equilibrium in the carbonate system that is linked to water pH. Carbon dioxide from the environment and silicate mineral weathering could both contribute to the increased bicarbonate ion (Egbueri, 2022; Saha et al., 2019). Increased bicarbonate ion levels were likely due to the process of respiration and decomposition of dead plant bodies during the dry season (Manea et al., 2019). All sample stations, bicarbonates (610 mg/L) were within the FAO irrigation threshold during both seasons.

3.1.7. Total hardness (TH)

Total hardness readings ranged from 58 (T1) to 106.7(W4) mg/L and 26.7 (T1) to 55.3(W5) mg/L during the wet and dry seasons, respectively (Table 4). During the wet season, stream flow rates increased, resulting in the lowest mean. The lowest TH value during the dry season could be due

Table 5. Variable loadings on varimax rotated factors in both wet and dry seasons.

Parameters	Rainy season		Dry season			
	PC1	PC2	PC1	PC2	PC3	PC4
Temperature	.362	.743			.897	
pH		-.935				.968
EC	.584	.707	.798	.415	.325	
TDS	.605	.675	.802	.429		
TH	.608	.681	.686	.451	.425	
Ca	.567	.700		.821	.436	
Mg	.913		.873			
Na	.984		.724		.593	
K	.496	.776	.444			.547
SO4	.662	.628	.872			
HCO3	.827	.303	.541	-.481	.537	
Cl	.749	.629		.964		
Eigen Value	10	1.5	7	2	1.7	1.5
% Variance	71.866	12.988	51.31	16.044	11.799	9.04
Cumulative Variance	71.866	84.85	51.31	67.354	79.153	88.192

Note: PC = Principal component.

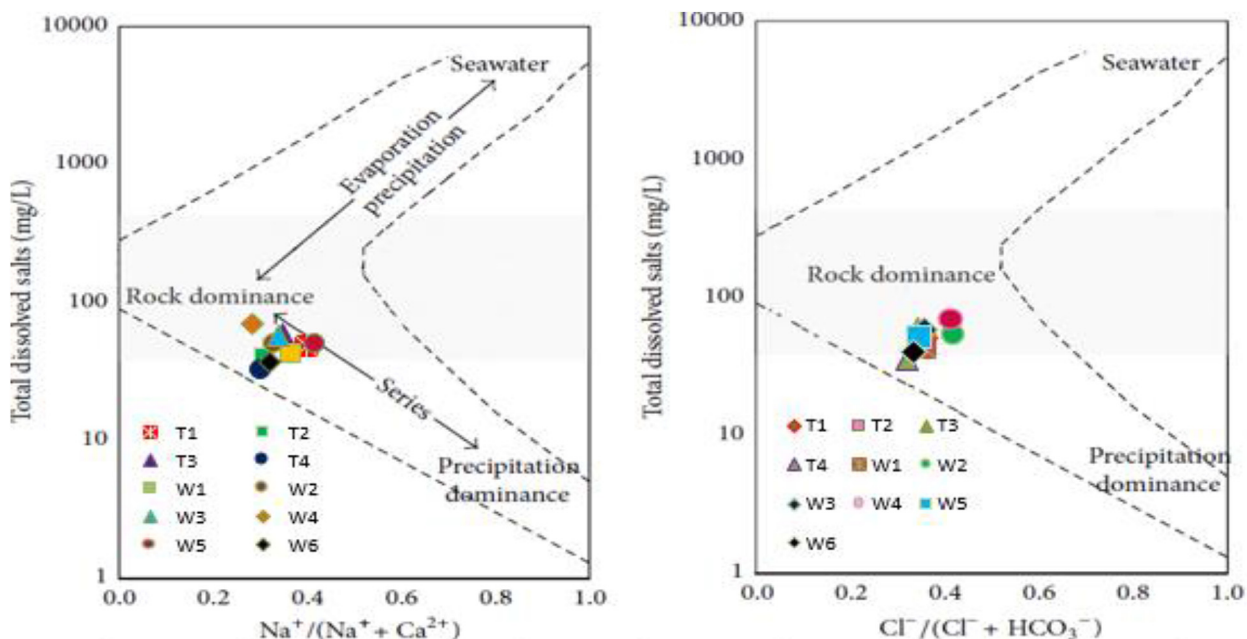


Figure 2a. Gibbs diagram for the wet season.

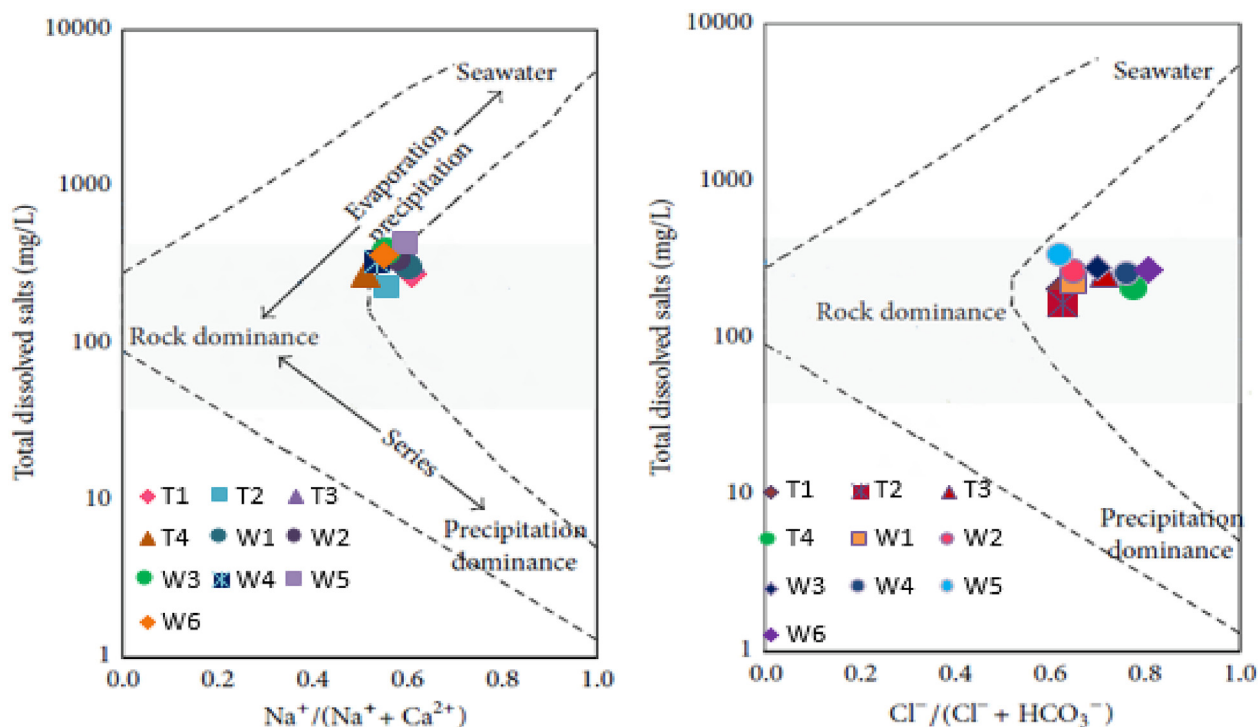


Figure 2b. Gibbs diagram for the dry season.

to low calcium and magnesium ions in the river water (Qureshimatva and Maurya, 2015). Rock weathering, waste from construction sites, vehicle wash facilities, and leachate could all have contributed to the highest levels found at sampling point W4 (Ameen, 2019).

3.1.8. Heavy metals

The cadmium, copper, and zinc concentrations ranging from 0.005 (T2) to 0.032 (W4) and 0.003 (T2 and T4) to 0.01 (W5) mg/L, 0.18 (T1) to 0.6 (W4) and 0.11 (T1) to 0.32 (W5) mg/L, and 0.08 (T4) to 0.271 (W5)

and 0.048 (T1) to 0.214 (W5) mg/L during wet and dry seasons, respectively (Table 4). In addition to these pollution parameters, the values of the other parameters have grown in the downstream zone (Ustaoglu et al., 2021). The highest value seen during the rainy season could be due to runoff from urban areas, agricultural areas, and land fill sites mixing with river water (Eliku and Leta, 2018; Tadesse et al., 2018). The dry season, on the other hand, was caused by low river water volume and flow (Edokpayi et al., 2017). Additionally, the subsequent release of metal ions could account for the highest value in the dry sampling event

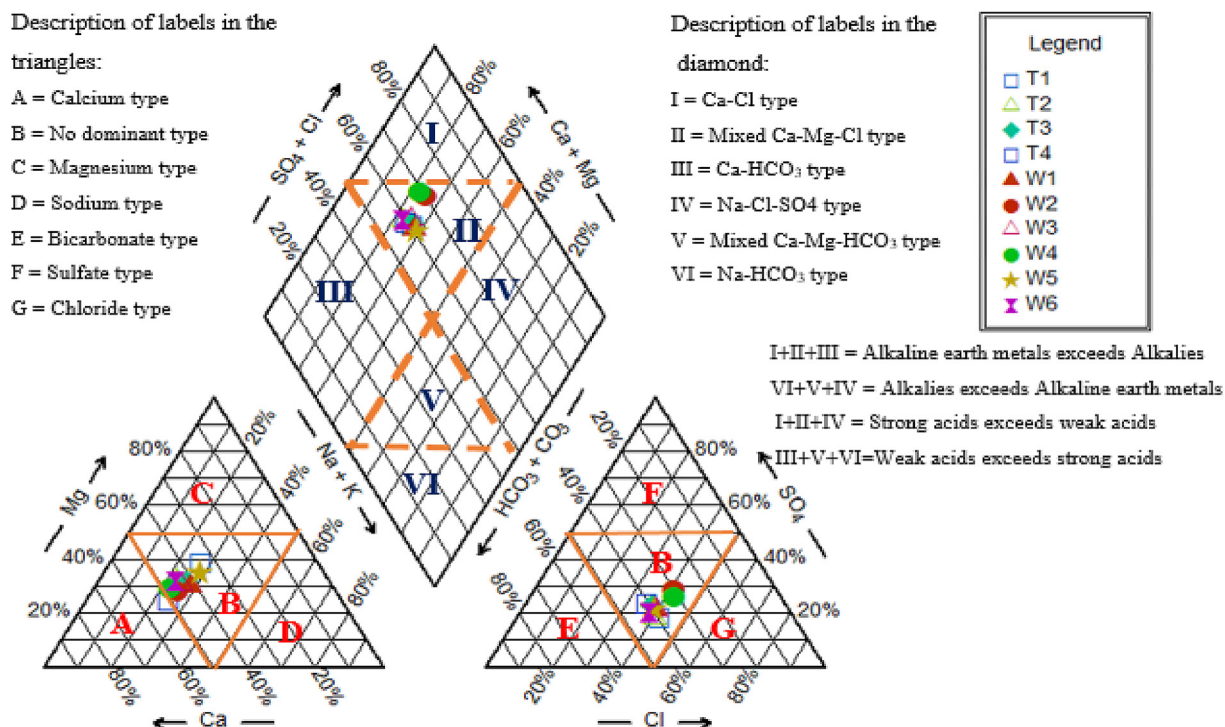


Figure 3a. Piper Diagram for wet seasons.

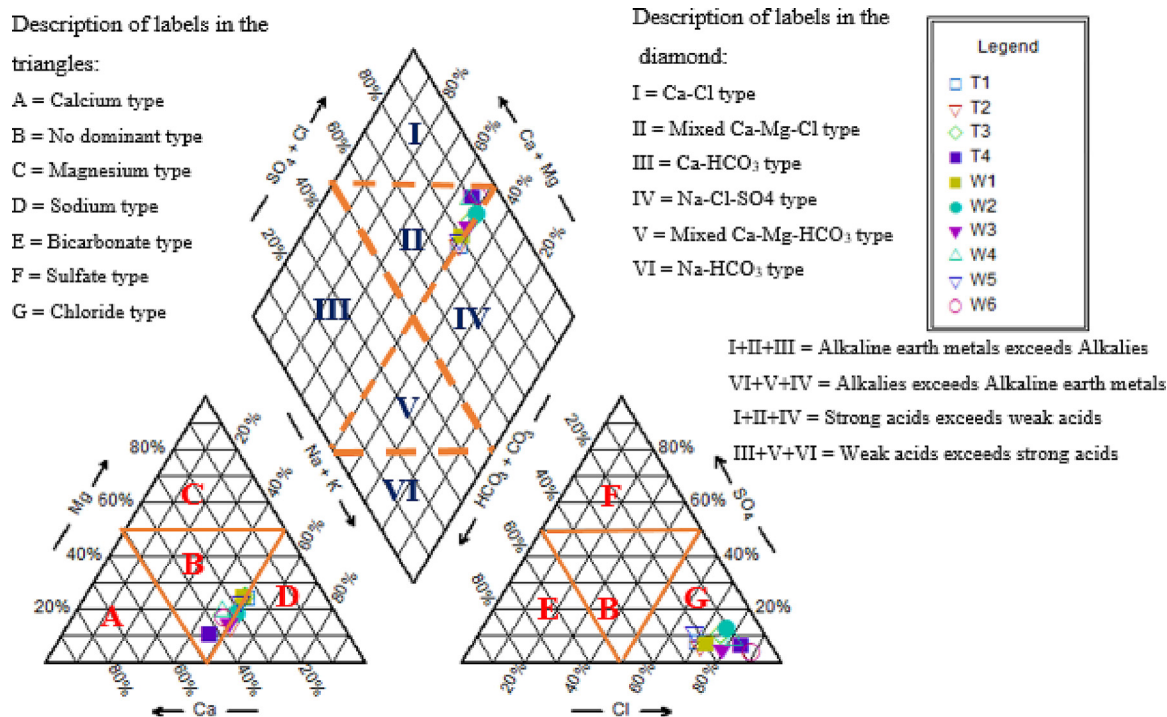


Figure 3b. Piper diagram for dry seasons.

(Manea et al., 2019). There is a rising amount of pollution in the downstream zone as a result of municipal, agricultural, and leachate drainage systems emptying into the Wabe River (Ustaoglu et al., 2021). However, all heavy metal concentration levels were safe during both seasons, with the exception of cadmium in W2, W4, W5, and W6 in wet seasons, according to FAO irrigation guidelines. Once heavy metal concentrations in urban rivers reach unsafe levels, both river creatures and people may experience long-term health risks (Töre et al., 2021).

### 3.2. Source of water pollution

The KMO test result was 0.8, and the Bartlett's sphericity test was done at 0.001 and 0.05 significance levels, indicating that the data is sufficient for PCA. Based on loading variables, water quality data was used in a main component analysis with an Eigen value of >1 to identify pollution sources in the Wabe River (Mustapha et al., 2011). There are factor loadings that are strong (>0.75), medium (0.5–0.75), and

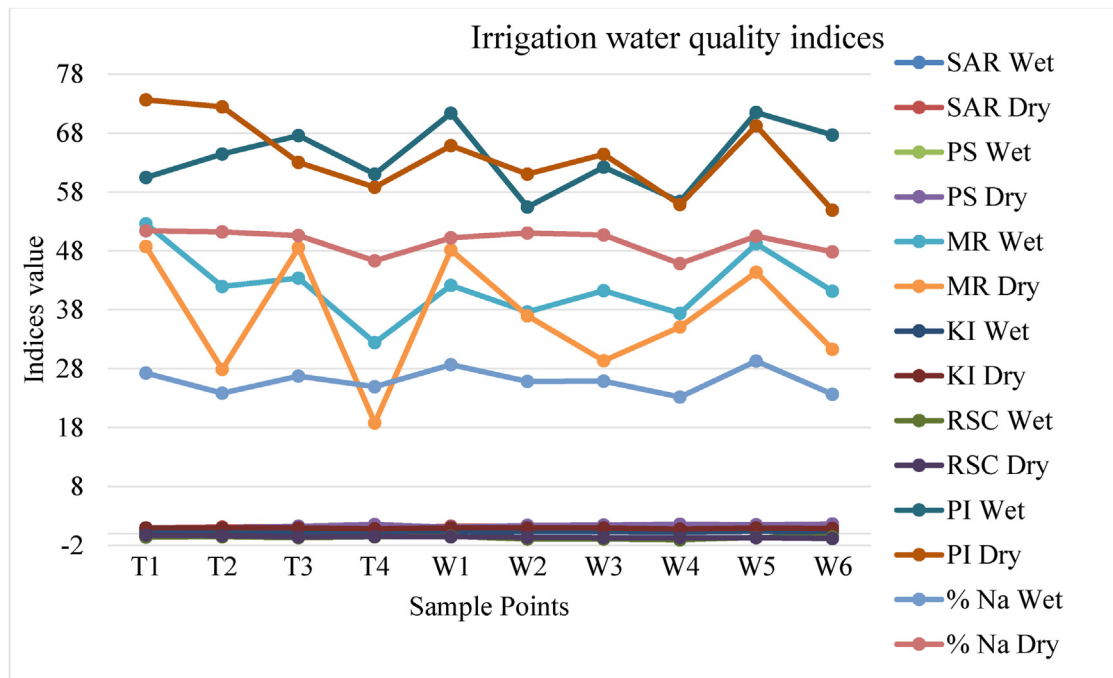


Figure 4a. Irrigation water quality indices.

moderate (0.3–0.5) (Egbueri et al., 2022). Two and four components of datasets are generated during the wet and dry seasons, respectively (Table 5).

3.2.1. Pollution source identification during the wet season

PC1's overall variance was 71.866 percent during the rainy season. This indicates that the magnesium, sodium, and bicarbonate ions are positively charged. Weathering of silicate and carbonate minerals, dissolved minerals in sedimentary rocks, and leaching from the soil surface

during rainstorms were all possible sources of ionic concentrations for the first component (PC1) (Egbueri et al., 2022; Nguyen et al., 2020). PC1 also has medium loading scores for EC, TH, TDS,  $Ca^{2+}$ ,  $SO_4^{2-}$ , and  $Cl^-$ . Sulphates, chlorides, bicarbonates of calcium and magnesium are common salts found in subsurface drainage water. These salts may found in tail water, though in considerably lower amounts than in drainage water. Based on the results of the factor analysis and common sources of water pollution, PC1 can be characterized as the 'agricultural use' factor with the presence of  $Ca^{2+}$  and  $Mg^{2+}$  (Boyacioglu, 2006). Temperature and

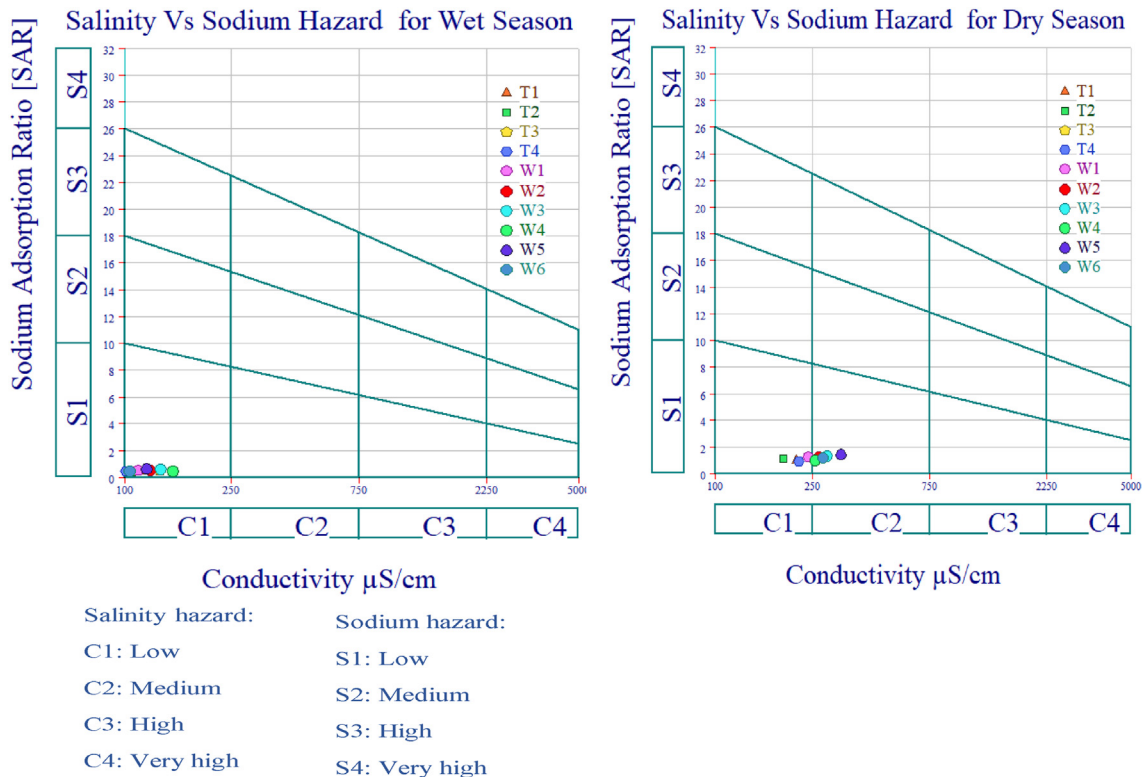


Figure 4b. Wilcox USSL diagram.

potassium both have modest loading values in PC1. PC2 has the highest potassium loading value (0.776) as well as high EC (0.707), TDS (0.675), total hardness (0.68), calcium (0.7), sulfate (0.628), and chloride (0.628) loading values plus a moderate loading value of temperature (0.743). The PC2 has a low bicarbonate loading value (0.303) (Table 5). Contributions from soil mineral dissolution in surface runoff and diluted wastewater inputs from residential areas could be indicated by this component (Matli and Nivedita, 2021). All of the aforementioned metrics may have increased due to the sediment influx in the downstream zone (Ustaoglu et al., 2021).

3.2.2. Pollution source identification during the dry season

Statistical study based on factor analysis discovered four components for the dry season water quality dataset. The first component (PC1) has a strong positive loading score on EC (0.798), TDS (0.802), magnesium (0.873), and sulfate (0.872). PC1 has a moderate loading score of TH (0.686), sodium (0.724), and bicarbonate (0.541). Furthermore, potassium has a loading value of 0.444, which is low (Table 5). The reduction in river water volume and the release of ions from bottom deposits have had a significant impact on the ionic content in the research region during the dry season. As a result, these parameters highlight the impact of desorption on the ionic composition of river water (Egbueri et al., 2021; Aydin et al., 2020).

The calcium (0.821) and chloride (0.964) loading values of the second component (PC2) are both significantly positive. The ionic exchange process happens within river water during the dry season, resulting in a rise in calcium and chloride concentrations (Aliyu et al., 2020). As a result, this component reveals the repercussions of the natural process

occurring inside the river water. The third (PC3) and fourth (PC4) components have significant positive loading values for temperature (0.897) and pH (0.968). The suspended particulates in river water may absorb sunlight during the dry season, elevating the temperature of the water (Ustaoglu and Tepe, 2019; Mustapha et al., 2013). pH fluctuations will be influenced by CO<sub>2</sub> removal from photosynthesis via bicarbonate degradation, salinity decrease from freshwater input, and organic matter degradation (Hamid et al., 2020).

3.3. Hydrochemical characteristics of the river water

3.3.1. Sources and Influencing factors for major ions

All samples from the Wabe River were concentrated in the dominant area of rock weathering during the wet season samples in the Gibbs diagram, which might be attributed to ionic composition in river water (Figure 2a). The dry season, the Gibbs diagram revealed two patterns. The remaining samples were concentrated in the first pattern, between rock dominance and the evaporation zone, with T2, W1, and T1 outside of the broken line. When sample locations occur between the rock dominance and evaporation zones, a mixed regulating mechanism (rock weathering and evaporation both played a role) is revealed (Wu et al., 2015). Cation exchange, evaporation, and human factors were all aspects that contributed to this pattern. Because of the general ionic content of river water, all samples were concentrated outside of the broken line (Figure 2b) (Jiang et al., 2020). The atmospheric precipitation zone is located in the lower right corner of the Gibbs diagram, when the water sample point's TDS values are low and Na<sup>+</sup>/(Na<sup>+</sup> + Ca<sup>2+</sup>) or Cl<sup>-</sup>/(Cl<sup>-</sup> + HCO<sub>3</sub><sup>-</sup>) is high. The rock weathering zone lies to the left of the centre on the Gibbs diagram,

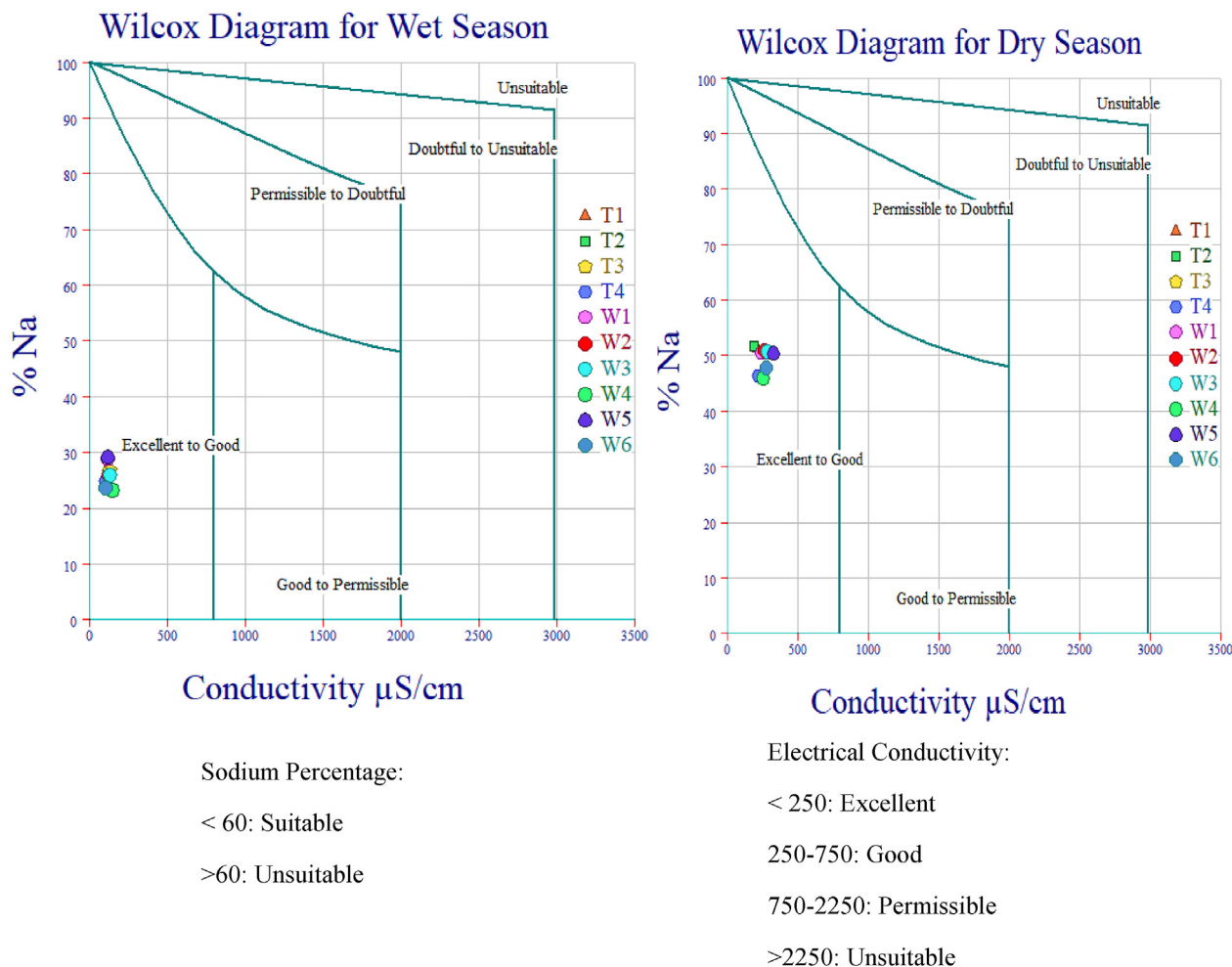


Figure 5. Wilcox diagram during wet and dry seasons.

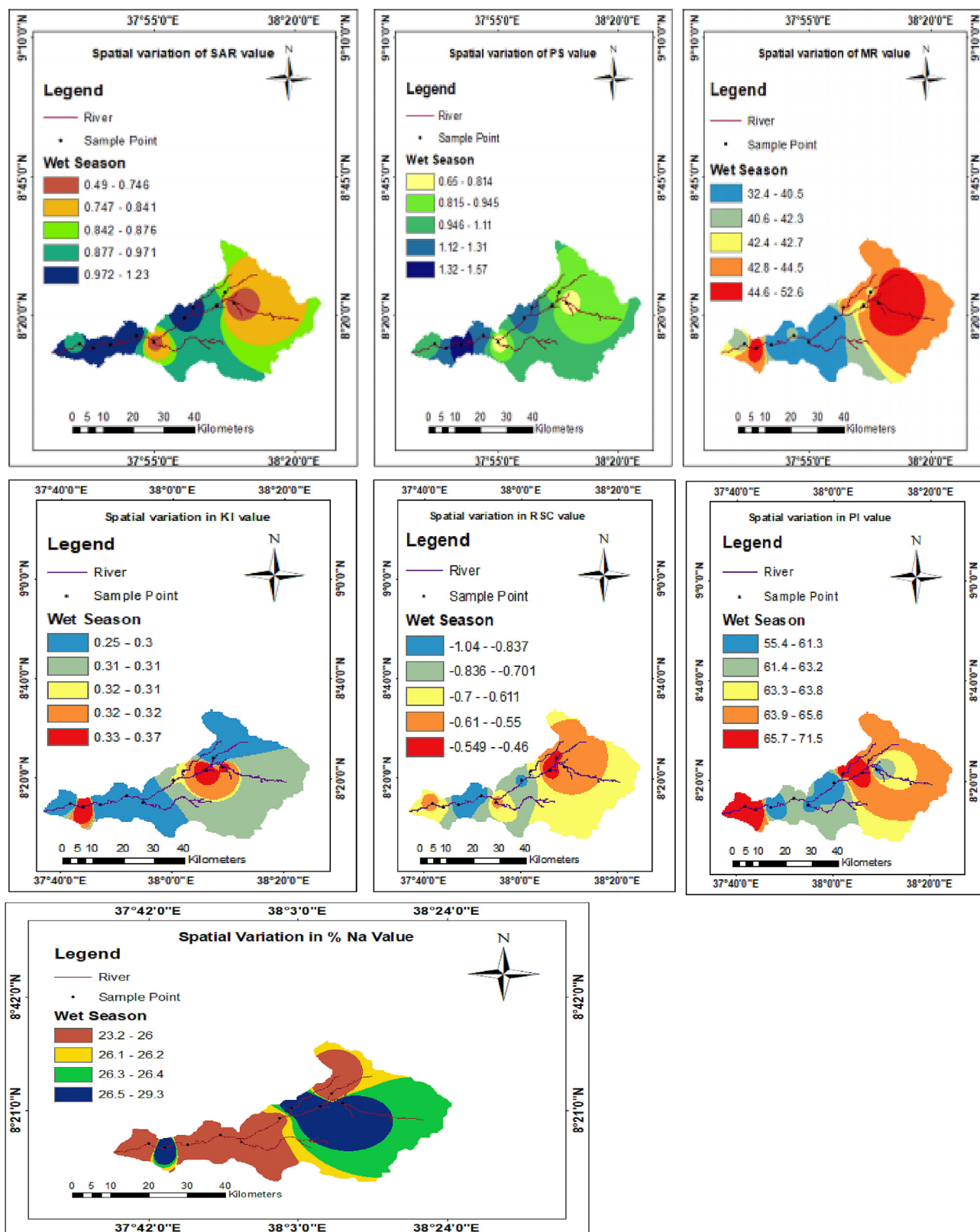


Figure 6. IDW map of irrigation water quality indices for wet season.

with a water sample with a medium TDS value and a  $\text{Na}^+ / (\text{Na}^+ + \text{Ca}^{2+})$  or  $\text{Cl}^- / (\text{Cl}^- + \text{HCO}_3^-)$  ratio of roughly 0.5. The water sample point in the upper right, on the other hand, is part of the evaporation concentration zone, which has high TDS and high  $\text{Na}^+ / (\text{Na}^+ + \text{Ca}^{2+})$  or  $\text{Cl}^- / (\text{Cl}^- + \text{HCO}_3^-)$  values (Omeka et al., 2022; Jiang et al., 2020).

### 3.3.2. Hydrochemical compositions and water type

All sample site data was grouped in Zone II of Piper diagrams over both seasons (Figure 3a and 3b). This indicates a higher concentration of alkali earth elements. The left and right side triangles revealed that all of the samples fell within the no dominant type zone during the rainy

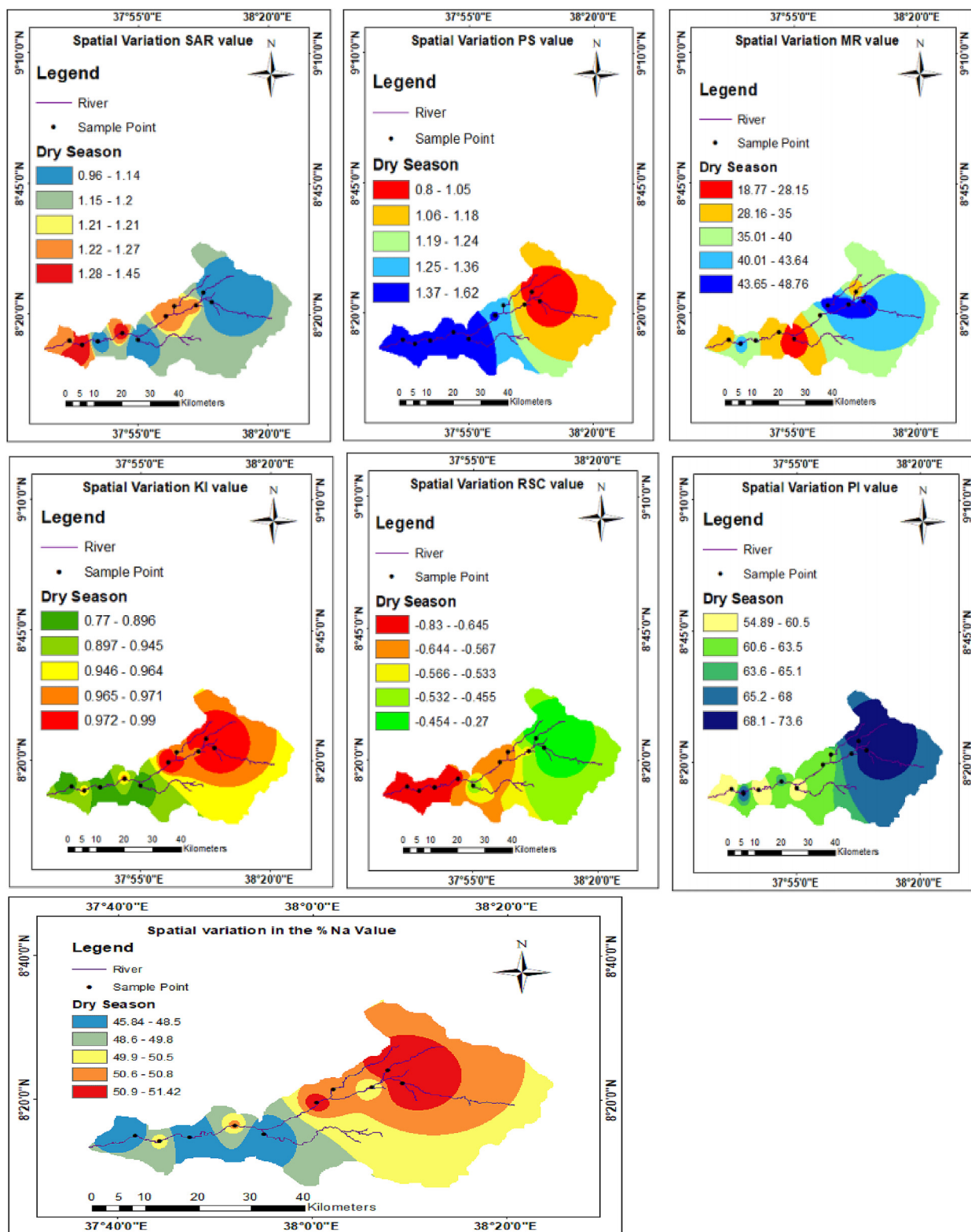


Figure 7. IDW map of irrigation water quality indices for dry season.

season, indicating that neither cations nor anions were dominant. All sample sites in the left side triangle fell into the no dominant type zone during the dry season, whereas all sample points in the right-side triangle fell into the Chloride type zone (Egbueri et al., 2021). This could be attributed to increased dissolved salts content and reduced water volume due to evaporation during the dry season (Aliyu et al., 2020). The piper diagrams demonstrated that the Wabe river water had a

calcium-magnesium-chloride hydro-chemical composition during both seasons. It's probable that the ion exchange mechanism in river water is to blame (Ouarani et al., 2020). Zones I, II, and IV are formed when strong acid concentrations outnumber weak acid concentrations (Egbueri et al., 2021).

During the rainy season, the left and right-side triangles revealed that every sample point was in the no dominant type zone, indicating that

neither cations nor anions were dominant. On the piper diagram for the dry sampling event, the left side triangle indicated that all sample points were in the no dominant type zone, whereas the right-side triangle indicated that all sample points were in the chloride type zone, indicating that chloride was the dominant ion from those anions during the dry season (Egbueri et al., 2021). A fast rate of evaporation leads dissolved salts in river water to concentrate during the dry season, resulting in chloride ions dominating anions (Aliyu et al., 2020).

### 3.4. River water evaluation for irrigation purposes

#### 3.4.1. Sodium adsorption ratio (SAR)

The current study obtained SAR values in the range of 0.49–1.23 meq/L and 0.99–1.45 meq/L during the wet and dry seasons, respectively, which are less than 20 meq/L, indicating that river water is suitable for irrigation (Figure 4a) (Ezugwu et al., 2019). Water samples T3, W2, W3, W4, W5, and W6 fell into the C2 S1 class during the dry season, indicating intermediate salinity and low sodium hazard water type, whereas the others fell into the C1 S1 class, indicating low salinity and low sodium hazard water type (Figure 4b). The Wilcox Salinity vs Sodium Hazard graph demonstrated that the measured Wabe River water at each station fell into the C1 S1 class during the rainy seasons, suggesting low salinity and sodium hazard water. The Wilcox diagram and the calculated SAR values confirmed that the river water is suitable for agriculture. For both seasons, an IDW interpolation map revealed the spatial variance of SAR values (Figures 6 and 7).

#### 3.4.2. Potential salinity (PS)

The potential salinity levels of Wabe river water samples ranged from 0.65 to 1.57 meq/L and 0.8–1.62 meq/L throughout the rainy and dry seasons, respectively (Figure 4a). The potential salinity values were below 3 meq/L at all test sites, indicating that the Wabe river water is appropriate for irrigation during both seasons (Berhe, 2020; Egbueri et al., 2021). All of the water sources investigated would present a low salinity threat when used for irrigation. The salinity hazard estimations also suggest that crops that are very sensitive to high salinity levels can be successfully grown in the research region (Figure 4b) (Egbueri et al., 2021). An IDW interpolation map was used to show the variability of PS values at all sampling points in both seasons (Figures 6 and 7).

#### 3.4.3. Magnesium ratio (MR)

One of the indications used to determine if water is suitable for irrigation is the magnesium ratio. With a higher magnesium ratio, the appropriateness will be diminished. During the rainy and dry seasons, the magnesium ratios were 32.41–52.6 and 18.77 to 48.76, respectively

(Figure 4a). A magnesium ratio of more than 50% is unacceptably high for irrigation (Egbueri et al., 2021; Berhe, 2020). During the wet season, all sample sites except T1 were below 50%, and during both seasons, all sample sites were below 50%. According to MR findings, Wabe water is appropriate for irrigation purposes.

#### 3.4.4. Kelly Index (KI)

During the wet and dry seasons, the Kelly Index values ranged from 0.25 to 0.37 and 0.77 to 0.99, respectively (Figure 4a). If one of Kelly's indices is more than one, the water contains too much sodium and is unfit for irrigation (Berhe, 2020). The Kelly index readings were less than one (KI1), indicating that the water from the Wabe River is acceptable for irrigation. The IDW maps showed how the KI value changed over time in both seasons (Figures 6 and 7). During both seasons, all GIS calculated and interpolated values were less than one at all sampling sites, indicating that river water quality was satisfactory.

#### 3.4.5. Residual sodium carbonate (RSC)

The concentration of bicarbonate and carbonate ions in water affects its suitability for irrigation. During the wet and dry seasons, RSC values in the Wabe river samples ranged from –1.04 to –0.46 meq/L and –0.83 to –0.27 meq/L, respectively (Figure 4a). Due to sodium carbonate, water with a high RSC has a high pH, and land irrigated with it becomes unproductive (Omeka et al., 2022; Joshi et al., 2009). Irrigation is appropriate when the RSC value is less than 1.25 meq/L. RSC values between 1.25 and 2.5 meq/L are considered marginal quality, whereas RSC values above 2.5 meq/L are not appropriate for irrigation (Berhe, 2020). During both seasons, IDW maps depicted the spatial fluctuation of RSC values (Figures 6 and 7). Both seasons had been calculated and interpolated in all of the samples, and RSC values were less than 1.25 meq/L, suggesting that the water quality was 'safe' for irrigation at all sampling locations. In water samples, RSC measurements were negative, indicating that calcium and magnesium ions had not precipitated out (Egbueri et al., 2021; Kumarasamy et al., 2014).

#### 3.4.6. Permeability Index (PI)

The Permeability Index readings for the wet and dry seasons, respectively, varied from 55.43 to 71.5 percent and 54.89 to 73.64 percent (Figure 4a). If the permeability index is less than 25, irrigation is not recommended. With permeability index values between 25 and 75, irrigation will be practicable. It is considered safe if the permeability index surpasses 75 (Berhe, 2020) proposing that all of the water sources sampled are appropriate for irrigation needs and won't negatively impact the soil permeability (Egbueri et al., 2021). All computed and interpolated permeability index values in both seasons and at each sample site

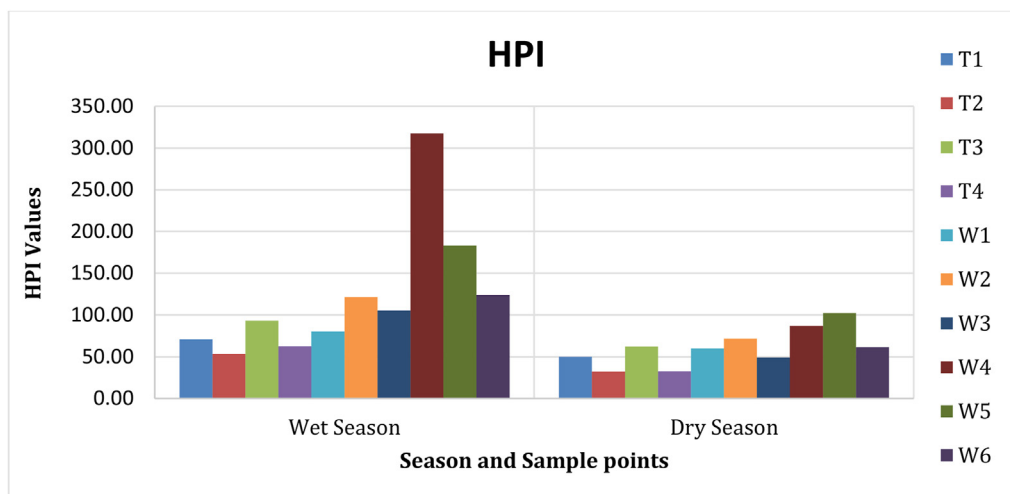


Figure 8a. Irrigation water quality indices.

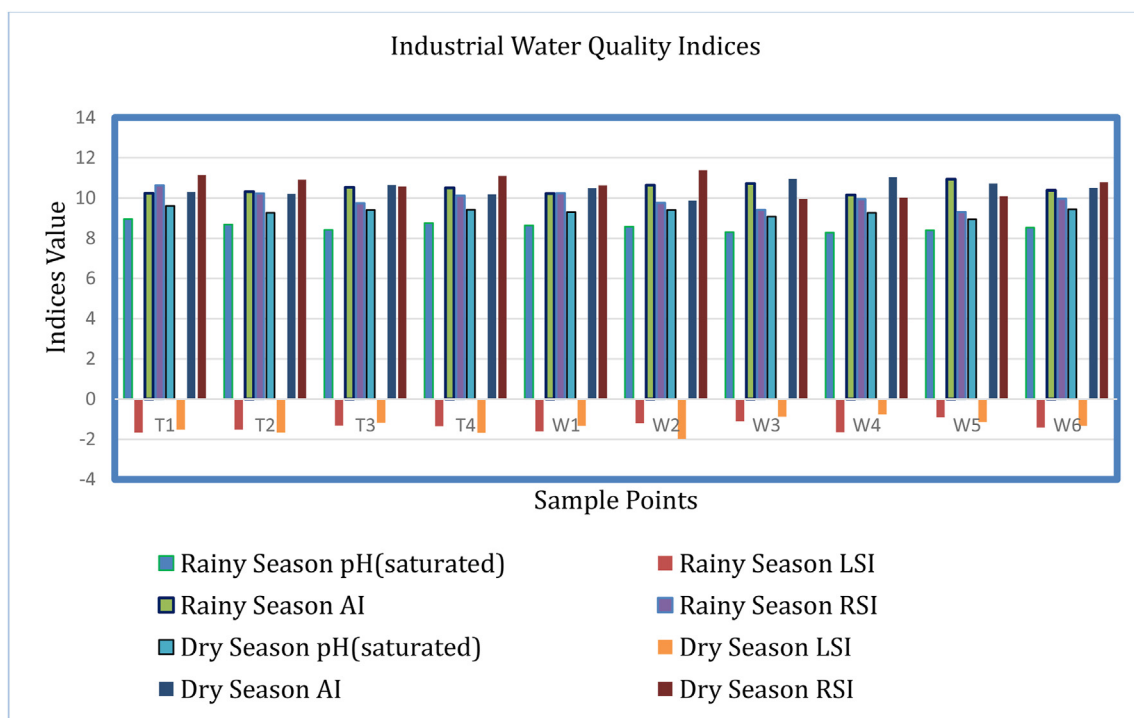


Figure 8b. Industrial water quality indices.

are classified as excellent in the permeability index classification. The IDW map illustrated the geographic changes in PI values during both seasons (Figures 6 and 7).

#### 3.4.7. Sodium percentage (% Na)

Sodium percentage (%Na) readings in the Wabe river water ranged from 23.18 to 29.29 during the wet season and 45.84 to 51.42 during the dry season, respectively (Figure 4a). In comparison to the dry season, the rainy season had the lowest sodium proportion. A sodium concentration of more exceeding 60% is not appropriate for irrigation, but less than 60% is acceptable for agricultural usage (Egbueri et al., 2021; Shil et al., 2019). Sodium percentages were less than 60% at all sampling sites during both seasons, indicating that river water could be used for agriculture. Irrigation water with increased sodium content has lower permeability. Similarly, the Wilcox diagram of electrical conductivity versus salt percent revealed that the river water was in excellent to good condition at all sample sites for both seasons (Figure 5).

#### 3.4.8. Heavy metal pollution index (HPI)

Three heavy metals (Copper, Cadmium and Zinc) were used to compute the HPI for irrigation utilizations. During the wet season, the computed heavy metal pollution index ranged from 53.34 (T2) to 317.58 (T3) (W4). HPI ranged from 32.24 (T2) to 102.42 (W5) during the dry season (Figure 8a). The wet season had the greatest HPI values, while the dry season had the lowest. Low concentrations of heavy metals caused the lowest HPI value in the upper stream of the river during both seasons. Whereas the highest value in the rainy season at W4 was due to leachate entry from nearby land fill site that contains heavy metals and that of the dry period at W5 was due to the retention of heavy metals in bottom sediments (Hamid et al., 2020). As per Biswas et al. (2017), the degree of pollution is said to be low if,  $HPI < 300$ , medium if  $300 < HPI < 600$ , and high if  $HPI > 600$ . Accordingly based on HPI, the degree of pollution of heavy metals was low in all sampling points except W4 (medium pollution) in the rainy season this might be due to absence of industries (Ustaoğlu et al., 2021). In general, river water was suitable for irrigation.

#### 3.5. River water quality evaluation for industrial purposes

To assess the suitability of the Wabe river water for industrial purposes can be utilized indices such as the Langelier Saturation Index (LSI), aggressive index (AI), and Ryznar Stability Index (RSI). The LSI values were in the range of  $-1.66$  to  $-0.9$  and  $-1.98$  to  $-0.76$  during the wet and dry seasons, respectively (Figure 8b). As a result, all computed values are in the range of  $-2$  to  $0$ , suggesting moderately aggressive water for industrial usage. The AI values were in the range of  $10.14$ – $10.93$  and  $9.87$  to  $11.02$  during the wet and dry seasons, respectively (Figure 8b). All river water samples were moderately aggressive for industrial use, except W2 in the dry season, which was highly aggressive. The Ryznar Stability Index (RSI) values at all sampling sites during both seasons were less than 9 (Figure 8b), indicating the river water was highly aggressive and corrosion is intolerable. However, the three indices' findings are crucially indicating that natural water resources are more corrosive than they are encrustation-prone. Several studies have reported similar findings in the literature (Abbasnia et al., 2018; Aghazadeh et al., 2017; Mankikar, 2021, Sajil Kumar, 2019; Egbueri, 2022) that water resources predict greater corrosion risks than scaling risks. This indicates the Wabe river water is not suitable for industrial process without treatment (Zhou et al., 2020).

#### 4. Conclusion

The properties of the Wabe River water contamination and its suitability for agricultural and industrial applications have been satisfactorily analyzed in-depth by the current investigation. According to the SAR, MP, PI, KI, PS, RSC, %Na, and HPI values, the Wabe river water is appropriate for agricultural use, with the exception of sampling point W4 during the rainy season due to a large input of residential wastewater from urban areas and leachate from a neighboring solid waste dumping site. According to the study's findings, farmers can use Wabe river water for their agricultural endeavors rather than solely relying on rainfall. According to the three indices, including the Langelier Saturation Index

(LSI), Aggressive Index (AI), and Ryznar Stability Index (RSI), Wabe River water was fairly aggressive for industrial use, with the exception of W2 (extremely aggressive) as per RSI. Since the water is corrosive, it must be purified before being used for industrial purposes. Additionally, to determine the hydrochemical composition of Wabe water, plot the piper diagrams; it is of the calcium-magnesium-chloride type. The Wabe River water contamination sources were located using Gibb's diagrams. All samples land in the rock weathering zone during the rainy season, indicating that geological structures and sediment influx are the sources of contamination. Gibb's diagrams during the dry season revealed that evaporation, cation exchange, anthropogenic activities, and bed rock degradation were the main sources of pollution. This study discovered that, in order to avoid contaminating the water in the Wabe River, the dumping site that is close to sample points W4 and W2 must be relocated. The river needs to be preserved and protected as a necessity.

## Declarations

### Author contribution statement

Tilahun Kasa, M Sc: Conceived and designed the experiments; Performed the experiments; Analyzed and interpreted the data; Contributed reagents, materials, analysis tools or data; Wrote the paper.

Abeanezer Lukas Bassa, M Sc: Analyzed and interpreted the data; Contributed reagents, materials, analysis tools or data.

Geleta Tilahun Negatu, M Sc; Zenebe Amele Sahile, M Sc: Performed the experiments; Contributed reagents, materials, analysis tools or data; Wrote the paper.

Daniel Reddythota, PhD: Conceived and designed the experiments; Analyzed and interpreted the data; Wrote the paper.

### Funding statement

This research did not receive any specific grant from funding agencies in the public, commercial, or not-for-profit sectors.

### Data availability statement

Data will be made available on request.

### Declaration of interest's statement

The authors declare no conflict of interest.

### Additional information

No additional information is available for this paper.

## Acknowledgements

The authors are grateful to the Ministry of Water, Irrigation & Energy, Addis Ababa, Ethiopia, for providing major secondary data.

## References

- Abbasia, A., Alimohammadi, M., Mahvi, A.H., Nabizadeh, R., Yousefi, M., Mohammadi, A.A., et al., 2018. Assessment of groundwater quality and evaluation of scaling and corrosiveness potential of drinking water samples in villages of Chabahr city, Sistan and Baluchistan province in Iran. *Data Brief* 16, 182–192.
- Aghazadeh, N., Chitsazan, M., Golestan, Y., 2017. Hydrochemistry and quality assessment of groundwater in the Ardabil area, Iran. *Appl. Water Sci.* 7 (7), 3599–3616.
- Aliyu, A.G., Jamil, N.R.B., Adam, M.B., bin, Zulkeflee, Z., 2020. Spatial and seasonal changes in monitoring water quality of Savanna River system. *Arabian J. Geosci.* 13 (2), 1–13.
- Ameen, H.A., 2019. Spring water quality assessment using water quality index in villages of Barwari Bala, Duhok, Kurdistan Region, Iraq. *Appl. Water Sci.* 9 (8), 1–12.
- Amit, S.K., Uddin, M.M., Rahman, R., Islam, S.M.R., Khan, M.S., 2017. A review on mechanisms and commercial aspects of food preservation and processing. *Agric. Food Secur.* 6 (1), 1–22.
- Angello, Z.A., Tränckner, J., Behailu, B.M., 2021. Spatio-temporal evaluation and quantification of pollutant source contribution in little Akaki river, Ethiopia: conjunctive application of factor analysis and multivariate receptor model. *Pol. J. Environ. Stud.* 30 (1), 23–34.
- APHA, 2012. Standards methods for the examination of water and wastewater. American Public Health Association. 23rd ed.
- Asnake, K., Worku, H., Argaw, M., 2021. Integrating river restoration goals with urban planning practices: the case of Kebena river, Addis Ababa. *Heliyon* 7 (7), e07446.
- Aydın, H., Ustaoglu, F., Tepe, Y., Soylu, E.N., 2020. Assessment of water quality of streams in northeast Turkey by water quality index and multiple statistical methods. *Environ. Forensics* 22 (1–2), 270–287.
- Berhe, B.A., 2020. Evaluation of groundwater and surface water quality suitability for drinking and agricultural purposes in Kombolcha town area, eastern Amhara region, Ethiopia. *Appl. Water Sci.* 10 (6), 1–17.
- Biswas, P.K., Uddin, N., Alam, S., Sultana, S., Ahmed, T., 2017. Evaluation of heavy metal pollution indices in irrigation and drinking water systems of barapukuria coal mine area, Bangladesh. *Am. J. Water Resour.* 5 (5), 146–151.
- Bouslah, S., Djemili, L., Houichi, L., 2017. Water quality index assessment of Koudiat Medouar Reservoir, northeast Algeria using weighted arithmetic index method. *J. Water Land Dev.* 35 (1), 221–228.
- Boyacioglu, H., 2006. Surface water quality assessment using factor analysis. *Water* 32 (3), 389–393.
- Child, D., 2006. *The Essentials of Factor Analysis*. A&C Black.
- CSA (Central Statistics Agency), 2017. Ethiopian National Population and Housing Census. Central Statistical Agency, Addis Ababa, p. 385.
- Edo Harka, Arus, Jilo, Nurs Boru, Behulu, Fiseha, 2021. Spatial-temporal rainfall trend and variability assessment in the Upper Wabe Shebelle River Basin, Ethiopia: application of innovative trend analysis method. *J. Hydrol.: Reg. Stud.* 37, 100915.
- Edokpayi, J.N., Odiyo, J.O., Durwoju, O.S., 2017. Impact of wastewater on surface water quality in developing countries: a case study of South Africa. *Water Qual.*
- Egbueri, J.C., 2018. Assessment of the quality of groundwaters proximal to dumpsites in Awka and Nnewi metropolises: a comparative approach. *Int. J. Energy Water Res.* 2, 33–48.
- Egbueri, J.C., 2022. Predicting and analysing the quality of water resources for industrial purposes using integrated data-intelligent algorithms. *Groundwater Sustain. Dev.* 100794.
- Egbueri, J.C., Mgbenu, C.N., Chukwu, C.N., 2019. Investigating the hydrogeochemical processes and quality of water resources in Ojoto and environs using integrated classical methods. *Model. Earth Syst. Environ.* 5 (4), 1443–1461.
- Egbueri, J.C., Mgbenu, C.N., Digwo, D.C., Nnyigide, C.S., 2021. A multi-criteria water quality evaluation for human consumption, irrigation and industrial purposes in Umunya area, southeastern Nigeria. *Int. J. Environ. Anal. Chem.* 1–25.
- Egbueri, J.C., Enyigwe, M.T., Ayejoto, D.A., 2022. Modeling the impact of potentially harmful elements on the groundwater quality of a mining area (Nigeria) by integrating NSFQI, HERisk code, and HCs. *Environ. Monit. Assess.* 194 (3), 1–28.
- Eliku, T., Leta, S., 2018. Spatial and seasonal variation in physicochemical parameters and heavy metals in Awash River, Ethiopia. *Appl. Water Sci.* 8 (6), 177.
- Etteieb, S., Cherif, S., Tarhouni, J., 2017. Hydrochemical assessment of water quality for irrigation: a case study of the Medjerda River in Tunisia. *Appl. Water Sci.* 7 (1), 469–480.
- Ezugwu, C.K., Onwuka, O.S., Egbueri, J.C., Unigwe, C.O., Ayejoto, D.A., 2019. Multi-criteria approach to water quality and health risk assessments in a rural agricultural province, southeast Nigeria. *HydroResearch* 2, 40–48.
- FAO, 2015. Climate Change and Food Security: Risks and Responses. Food and Agriculture Organization of the United Nations.
- Ficklin, D.L., Stewart, I.T., Maurer, E.P., 2013. Climate change impacts on streamflow and subbasin-scale hydrology in the Upper Colorado River Basin. *PLoS One* 8 (8), e71297.
- Goher, M.E., Hassan, A.M., Abdel-Moniem, I.A., Fahmy, A.H., El-Sayed, S.M., 2014. Evaluation of surface water quality and heavy metal indices of Ismailia Canal, Nile River, Egypt. *Egypt. J. Aquat. Res.* 40 (3), 225–233.
- Hamid, A., Bhat, S.U., Jehangir, A., 2020. Local determinants influencing stream water quality. *Appl. Water Sci.* 10 (24), 1–16.
- Hasan, M., Ahmed, S., Adnan, R., 2020. Environmental and Sustainability Indicators Water quality indices to assess the spatiotemporal variations of Dhaleshwari river in central Bangladesh. *Environ. Sustain. Indic.* 8, 100068.
- Hatfield, J.L., Prueger, J.H., 2015. Temperature extremes: effect on plant growth and development. *Weather Clim. Extrem.* 10, 4–10.
- Jiang, Y., Gui, H., Yu, H., Wang, M., Fang, H., Wang, C., Chen, C., Zhang, Y., Huang, Y., 2020. Hydrochemical characteristics and water quality evaluation of rivers in different regions of cities: a case study of Suzhou city in Northern Anhui province, China. *Water* 12 (4), 1–22.
- Joshi, D.M., Kumar, A., Agrawal, N., 2009. Assessment of the irrigation water quality of river Ganga in Haridwar district. *Rasayan J. Chem.* 2 (2), 285–292.
- Kadam, A., Wagh, V., Jacobs, J., Patil, S., Pawar, N., Umrikar, B., Sankhua, R., Kumar, S., 2021. Integrated approach for the evaluation of groundwater quality through hydro geochemistry and human health risk from Shivganga river basin. *Environ. Sci. Pollut. Res.* Pune, Maharashtra, India 29 (3), 4311–4333. PMID: 34403054.
- Kumarasamy, P., Dahms, H.U., Jeon, H.J., Rajendran, A., Arthur James, R., 2014. Irrigation water quality assessment—an example from the Tamiraparani river, Southern India. *Arabian J. Geosci.* 7 (12), 5209–5220.
- Legese, K., Bekele, A., Kiros, S., 2019. A Survey of large and medium-sized mammals in Wabe forest fragments, Gurage zone, Ethiopia. *Int. J. Avian Wildlife Biol.* 4 (2), 32–38.

- Manea, M.H., Al-Tawash, B.S., Al-Saady, Y.I., 2019. Hydrochemical characteristics and evaluation of surface water of Shatt Al-Hilla, Babil Governorate, Central Iraq. *Iraqi J. Sci.* 60 (3), 583–600.
- Mankikar, T., 2021. Comparison of indices for scaling and corrosion tendency of groundwater: case study of unconfined aquifer from Mahoba District, UP State. *Appl. Water Sci.* 11 (6), 1–12.
- Manuel, R., Machado, A., Serralheiro, R.P., 2017. Soil salinity : effect on vegetable crop growth . Management practices to prevent and mitigate soil salinization. *Horticulture* 3 (30), 1–13.
- Matli, C.S., Nivedita, 2021. Water quality modelling of river mahanadi using principal component analysis (PCA) and multiple linear regression (MLR). *Int. J. Environ.* 10 (1), 83–98.
- Mekonnen, B., Haddis, A., Zeine, W., 2020. Assessment of the effect of solid waste dump site on surrounding soil and River Water quality in tepi town, southwest Ethiopia. *J. Environ. Public Health* 2020, 1–9.
- Menberu, Z., Mogesse, B., Reddythota, D., 2021. Evaluation of water quality and eutrophication status of Hawassa Lake based on different water quality indices. *Appl. Water Sci.* 11 (3), 1–10.
- Mukate, S., Panaskar, D., Wagh, V., Muley, A., Jangam, C., Pawar, R., 2017. Impact of anthropogenic inputs on water quality in Chincholi industrial area of Solapur, Maharashtra, India. *Groundwater Sustain. Dev.* 7, 359–371.
- Mustapha, A., Nabegu, A.B., Putra, U., State, K., 2011. Surface water pollution source identification using principal component and factor analysis in Getsi River, Kano, Nigeria. *Aust. J. Basic Appl. Sci.* 5 (12), 1507–1512.
- Mustapha, A., Aris, A.Z., Juahir, H., Ramli, M.F., Kura, N.U., 2013. River water quality assessment using environmental techniques: case study of Jakara River Basin. *Environ. Sci. Pollut. Control Ser.* 20 (8), 5630–5644.
- Namara, W.G., Hirpo, G.M., Feyissa, T.A., 2022. Evaluation of impact of climate change on the watershed hydrology, case of Wabe Watershed, Omo Gibe River basin, Ethiopia. *Arabian J. Geosci.* 15, 1356.
- Neina, D., 2019. The role of soil pH in plant nutrition and soil remediation. *Appl. Environ. Soil Sci.* 2019 (3), 5794869.
- Ngabirano, H., Byamugisha, D., Ntambi, E., 2016. Effects of seasonal variations in physical parameters on quality of gravity flow water in Kyanamira sub-county, Kabale district, Uganda. *J. Water Resour. Protect.* 8 (13), 1297–1309.
- Nguyen, T.H., Helm, B., Hettiarachchi, H., Caucci, S., Krebs, P., 2020. Quantifying the information content of a water quality monitoring network using principal component analysis: a case study of the freiberger mulde river basin, Germany. *Water* 12 (2), 420.
- Omeke, M.E., Egbueri, J.C., Unigwe, C.O., 2022. Investigating the hydrogeochemistry, corrosivity and scaling tendencies of groundwater in an agrarian area (Nigeria) using graphical, indexical and statistical modelling. *Arabian J. Geosci.* 15 (13), 1–24.
- Ouarani, M., Bahir, M., Mulla, D.J., Ouazar, D., Chehbouni, A., Dhiba, D., Ouhamdouch, S., El Mountassir, O., 2020. Groundwater quality characterization in an overallocated semi-arid coastal area using an integrated approach: case of the Essaouira basin, Morocco. *Water* 12 (11), 1–19.
- Parris, K., 2011. Impact of agriculture on water pollution in OECD countries: recent trends and future prospects. *Int. J. Water Resour. Dev.* 27 (1), 33–52.
- Preisner, M., 2020. Surface water pollution by untreated municipal wastewater discharge due to a sewer failure. *Environ. Process.* 7 (3), 767–780.
- Qureshimatva, U., Maurya, R., 2015. Determination of physico-chemical parameters and water quality index (Wqi) of chandlodia lake, Ahmedabad, Gujarat, India. *J. Environ. Anal. Toxicol.* 5 (4), 1000288.
- Rawat, K.S., Singh, S.K., Gautam, S.K., 2018. Assessment of groundwater quality for irrigation use: a peninsular case study. *Appl. Water Sci.* 8 (8), 1–24.
- Reddythota, Daniel, Timotewos, Mosisa Teferi, 2022. Evaluation of pollution status and detection of the reason for the death of fish in chamo lake, Ethiopia. *J. Environ. Public Health* 2022. Article ID 5859132, 12 pages.
- Saha, S., Reza, A.H.M.S., Roy, M.K., 2019. Hydrochemical evaluation of groundwater quality of the Tista floodplain, Rangpur, Bangladesh. *Appl. Water Sci.* 9 (8), 1–12.
- Sahle, M., Saito, O., Fürst, C., Yeshitela, K., 2019. Quantifying and mapping of water-related ecosystem services for enhancing the security of the food-water-energy nexus in tropical data-sparse catchment. *Sci. Total Environ.* 646, 573–586.
- Sajil Kumar, P.J., 2019. Assessment of corrosion and scaling potential of the groundwater in the Thanjavur district using hydrogeochemical analysis and spatial modeling techniques. *SN Appl. Sci.* 1 (5), 1–13.
- Şener, Ş., Şener, E., Davraz, A., 2017. Evaluation of water quality using water quality index (WQI) method and GIS in Aksu River (SW-Turkey). *Sci. Total Environ.* 584–585, 131–144.
- Shil, S., Singh, U.K., Mehta, P., 2019. Water quality assessment of a tropical river using water quality index (WQI), multivariate statistical techniques and GIS. *Appl. Water Sci.* 9 (7), 1–21.
- Sylus, K.J., Ramesh, H., 2018. Geo-statistical analysis of groundwater quality in an unconfined aquifer of Nethravathi and Gurpur river confluence, India. *Model. Earth Syst. Environ.* 4 (4), 1555–1575.
- Tadesse, M., Tsegaye, D., Girma, G., 2018. Assessment of the level of some physico-chemical parameters and heavy metals of Rebu river in oromia region, Ethiopia. *MOJ Biol. Med.* 3 (3), 99–118.
- Terfasa, F., Tilahun Daba, A., Pandian, M., 2019. Assessments of the total heterotrophic bacterial population density from Wabe River, south-Central Ethiopia. *Int. J. Innov. Pharm. Sci. Res.* 7 (1), 1–13.
- Töre, Y., Ustaoglu, F., Tepe, Y., Kalipci, E., 2021. Levels of toxic metals in edible fish species of the Tigris River (Turkey); threat to public health. *Ecol. Indic.* 123, 107361.
- Ustaoglu, F., Tepe, Y., 2019. Water quality and sediment contamination assessment of Pazarsuyu Stream, Turkey using multivariate statistical methods and pollution indicators. *Int. Soil Water Conserv. Res.* 7 (1), 47–56.
- Ustaoglu, F., Tepe, Y., Taş, B., 2020. Assessment of stream quality and health risk in a subtropical Turkey river system: a combined approach using statistical analysis and water quality index. *Ecol. Indic.* 113, 105815.
- Ustaoglu, F., Taş, B., Tepe, Y., Topaldemir, H., 2021. Comprehensive assessment of water quality and associated health risk by using physicochemical quality indices and multivariate analysis in Terme River, Turkey. *Environ. Sci. Pollut. Res.* 28 (44), 62736–62754.
- Wali, S.U., Alias, N., Harun, S Bin, 2020. Quality reassessment using water quality indices and hydrochemistry of groundwater from the Basement Complex section of Kaduna Basin, NW Nigeria. *Appl. Sci.* 2 (10), 1–21.
- Weldeyohannis, Y.H., Aneseyee, A.B., Sodango, T.H., 2020. Evaluation of current solid waste disposal site based on socio-economic and geospatial data: a case study of Wolkite Town, Ethiopia. *GeoJournal* 1–17.
- WHO (World Health Organization), 2008. Guidelines for drinking-water quality: second addendum. In: Recommendations, 1. World Health Organization.
- Wu, H., Chen, J., Qian, H., Zhang, X., 2015. Chemical characteristics and quality assessment of groundwater of exploited Aquifers in beijiao water source of yinchuan, China: a case study for drinking, irrigation, and industrial purposes. *J. Chem.* 2015, 726340.
- Zaman, M., Shahid, S.A., Heng, L., 2018. Guideline for Salinity Assessment, Mitigation and Adaptation Using Nuclear and Related Techniques. Springer Nature Switzerland AG.
- Zhou, M., Li, X., Zhang, M., Liu, B., Zhang, Y., Gao, Y., et al., 2020. Water quality in a worldwide coal mining city: a scenario in water chemistry and health risks exploration. *J. Geochem. Explor.* 213, 106513.